Two Classes of Gap Junction Channels Mediate Soma-Germline Interactions Essential for Germline Proliferation and Gametogenesis in *Caenorhabditis elegans*

Todd A. Starich,* David H. Hall,† and David Greenstein*,[1]
*Department of Genetics, Cell Biology, and Development, University of Minnesota, Minneapolis, Minnesota 55455, and †Department of Neuroscience, Albert Einstein College of Medicine, Bronx, New York 10461
ORCID ID: 0000-0001-8189-2087 (D.G.)

ABSTRACT In all animals examined, somatic cells of the gonad control multiple biological processes essential for germline development. Gap junction channels, composed of connexins in vertebrates and innexins in invertebrates, permit direct intercellular communication between cells and frequently form between somatic gonadal cells and germ cells. Gap junctions comprise hexameric hemichannels in apposing cells that dock to form channels for the exchange of small molecules. Here we report essential roles for two classes of gap junction channels, composed of five innexin proteins, in supporting the proliferation of germline stem cells and gametogenesis in the nematode *Caenorhabditis elegans*. Transmission electron microscopy of freeze-fracture replicas and fluorescence microscopy show that gap junctions between somatic cells and germ cells are more extensive than previously appreciated and are found throughout the gonad. One class of gap junctions, composed of INX-8 and INX-9 in the soma and INX-14 and INX-21 in the germ line, is required for the proliferation and differentiation of germline stem cells. Genetic epistasis experiments establish a role for these gap junction channels in germline proliferation independent of the *glp-1/Notch* pathway. A second class of gap junctions, composed of somatic INX-8 and INX-9 and germline INX-14 and INX-22, is required for the negative regulation of oocyte meiotic maturation. Rescue of gap junction channel formation in the stem cell niche rescues germline proliferation and uncovers a later channel requirement for embryonic viability. This analysis reveals gap junctions as a central organizing feature of many soma–germline interactions in *C. elegans*.

SOMATIC cells function at multiple levels to promote the development of the germ line and enable its reproductive functions. Enrico Sertoli first deduced the importance of soma–germline interactions in his description of the branched cells in the testis that bear his name, calling them "mother cells" for their intuited role in nursing the germ cells (Sertoli 1865). He correctly recognized that the Sertoli cells are not progenitors of the spermatozoa, but are instead necessary for their proper development. Sertoli cells exemplify the involvement of somatic cells in the multiple events characteristic of germline development in general, including the specification of the sexual fate of the germ line and supporting cells of the gonad; the self-renewal and differentiation of germline stem cells in the niche; and the development and maturation of functional gametes (reviewed by Oatley and Brinster 2012; Svingen and Koopman 2013). Cells of the somatic gonad often carry out several stage-specific functions in germline development. Thus, genetic studies have been influential for teasing apart this biological complexity to reveal the mechanisms by which soma–germline interactions control reproductive processes.

The nematode *Caenorhabditis elegans* provides a genetic paradigm for the analysis of soma–germline interactions (reviewed by Hubbard and Greenstein 2000; Kimble and Crittenden 2007; Hansen and Schedl 2013; Hubbard *et al.* 2013). The somatic distal tip cell (DTC) constitutes a niche for the maintenance of the germline stem cell population (Figure 1). As germ cells move away from the DTC, they enter meiotic prophase I. Following exit from pachytene near the loop region,

doi: 10.1534/genetics.114.168815
Manuscript received July 28, 2014; accepted for publication September 6, 2014; published Early Online September 6, 2014.
Available freely online through the author-supported open access option.
Supporting information is available online at http://www.genetics.org/lookup/suppl/doi:10.1534/genetics.114.168815/-/DC1.
[1]Corresponding author: Department of Genetics, Cell Biology, and Development, University of Minnesota, 4-208 MCB, 420 Washington Ave., SE, Minneapolis, MN 55455. E-mail: green959@umn.edu

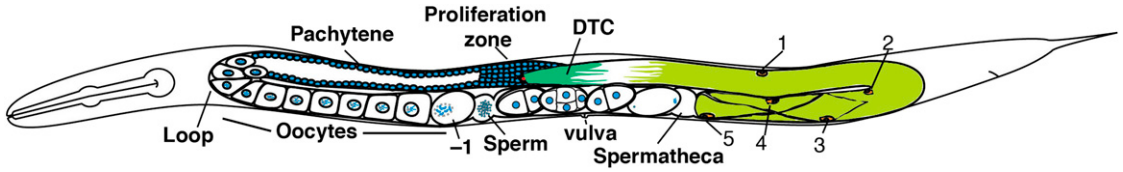

Figure 1 Representation of the adult hermaphrodite gonad. Germ cells are shown in the left arm, and somatic cells are shown in the right arm, although both tissues exist in the two arms. Germ cells progress distally to proximally from mitotic proliferation through early stages of meiotic prophase (left) and are in contact with the somatic DTC or sheath cells (right). One of each pair of sheath cell nuclei is shown; the boundary between sheath cell 1 and 2 is not indicated.

germ cells differentiate as spermatocytes in the L4 larval stage and as oocytes in adults. Oogenesis progresses to the diakinesis stage in the proximal gonad arm, and the most proximal (–1) oocyte undergoes meiotic maturation in response to the major sperm protein (MSP) hormone (McCarter *et al.* 1999; Miller *et al.* 2001). Meiotic maturation is defined by the transition to metaphase I, signified by nuclear envelope breakdown, rearrangement of the cortical cytoskeleton, and meiotic spindle assembly. The mature oocyte is then ovulated and fertilized.

Laser ablation of the DTC causes all germ cells to enter the meiotic pathway of development (differentiation), resulting in the loss of stem cells (Kimble and White 1981). The DTC promotes germline proliferation and inhibits entry into the meiotic pathway by activation of GLP-1/Notch signaling in the germ line (Austin and Kimble 1987, 1989; Yochem and Greenwald 1989). The Delta/Serrate/LAG-2 (DSL)-family ligands LAG-2 and APX-1 expressed in the DTC activate GLP-1/Notch signaling in the germ line (Henderson *et al.* 1994; Tax *et al.* 1994; Fitzgerald and Greenwald 1995; Nadarajan *et al.* 2009). In the absence of *glp-1* function, only approximately four to eight germ cells are produced and develop as functional sperm (Austin and Kimble 1987).

GLP-1 functions together with the LAG-1 CSL and SEL-8/LAG-3 mastermind transcription factors (Christensen *et al.* 1996; Tax *et al.* 1997; Doyle *et al.* 2000; Petcherski and Kimble 2000) and regulates transcription of genes needed for the maintenance of germline stem cells, including *sygl-1* and *lst-1*, whose mechanisms of action are unknown (Kershner *et al.* 2014). GLP-1/Notch signaling negatively regulates the activity of the GLD-1 and GLD-2 pathways (Francis *et al.* 1995a,b; Kadyk and Kimble 1998; Hansen *et al.* 2004a,b), which promote meiotic entry through the regulation of messenger RNA (mRNA) translation (reviewed by Hansen and Schedl 2013). In the absence of *gld-1* and *gld*-2 activity, *glp-1* is dispensable for germline proliferation (Kadyk and Kimble 1998; Hansen *et al.* 2004a,b). Whereas *glp-1/Notch* signaling is required for germline proliferation, other genetic pathways modulate proliferation control in response to changes in environmental conditions or the availability of nutrients (reviewed by Hubbard *et al.* 2013). These include the AMP-activated protein kinase, insulin/IGF signaling, TOR–S6 kinase, and TGF-β pathways (Narbonne and Roy 2006; Michaelson *et al.* 2010; Dalfó *et al.* 2012; Korta *et al.* 2012). In favorable growth environments (*e.g.*, abundant food and low population densities), the ASI sensory neuron secretes the DAF-7 TGF-β ligand, which acts on the DTC to promote expansion of the larval germline stem cell population (Dalfó *et al.* 2012). TGF-β signaling influences the proliferation *vs.* differentiation decision of germline stem cells in parallel to the GLP-1/Notch pathway. Thus, the niche responds to systemic cues to control germline stem cells, but how this information is communicated from the soma to the germ line is not understood.

Extensive laser ablation experiments identified soma–germline interactions mediated by cells of the gonadal sheath and spermathecal cell lineages in multiple germline processes (McCarter *et al.* 1997; Killian and Hubbard 2005). Ablation of both sheath-spermathecal precursor (SS) cells in a gonad arm resulted in a significant reduction in germline proliferation (McCarter *et al.* 1997). Ablation of both SS cells in a gonad arm in the gain-of-function *glp-1(oz112)* genetic background, in which GLP-1/Notch signaling is ligand-independent and constitutive (Berry *et al.* 1997), reduced germline proliferation (McCarter *et al.* 1997). This result indicated that the SS cells or their descendants support germline proliferation independently of GLP-1/Notch signaling. Among the SS cell progeny, the distal pair of sheath cells was shown to carry most of the proliferation-promoting function (Killian and Hubbard 2005).

Laser ablation of a single SS cell eliminates five gonadal sheath cells and nine spermathecal cells in that gonad arm and results in ovulation defects. Interactions between follicle-like gonadal sheath cells and oocytes regulate meiotic maturation. In the absence of sperm, as occurs in germline-feminizing genetic backgrounds or upon sperm depletion through self-fertilization, oocytes arrest in the diakinesis stage of meiotic prophase I. The proximal gonadal sheath cells appear to function as the chief MSP sensors. Protein kinase A (PKA) signaling in the sheath cells is required for all MSP responses in the germ line (Govindan *et al.* 2006, 2009; Harris *et al.* 2006; Cheng *et al.* 2008; Jud *et al.* 2008; Nadarajan *et al.* 2009; Kim *et al.* 2012). Inhibitory G-protein signaling in the gonadal sheath cells is required to prevent PKA signaling and meiotic maturation when sperm are absent (Govindan *et al.* 2006, 2009). The gonadal sheath cells appear to inhibit meiotic maturation in part through the formation of gap junctions with oocytes (Hall *et al.* 1999; Govindan *et al.* 2006, 2009; Whitten and Miller 2007; Nadarajan *et al.* 2009). The sheath cells are analogous to cumulus granulosa cells in mammals, which form gap junctions with oocytes at transzonal projections (Anderson and Albertini 1976). Soma–germline gap

junctions also inhibit meiotic maturation and are targeted by upstream signaling in mammals (Norris *et al.* 2008, 2009; Vaccari *et al.* 2008; Robinson *et al.* 2012; Zhang *et al.* 2012; reviewed by Conti *et al.* 2012).

Innexins and connexins mediate gap junction communication in invertebrates and vertebrates, respectively (reviewed by Nielsen *et al.* 2012; Simonsen *et al.* 2014). Although unrelated by sequence, innexins and connexins are structurally and topologically similar and function in an analogous manner. Hexameric hemichannels assemble in opposing cells and associate (dock) at sites of close apposition to form channels through which small molecules and ions move (<2 kDa for innexin-containing gap junctions). Prior work identified the germline innexins INX-14 and INX-22 as negative regulators of oocyte meiotic maturation (Govindan *et al.* 2006, 2009; Whitten and Miller 2007). INX-14 and INX-22 were observed to colocalize to punctate structures throughout the germ line (Govindan *et al.* 2009), including distal regions in which gap junctions had not been previously described. Roles for *inx-14* in promoting germline proliferation (Govindan *et al.* 2009) and sperm guidance from the uterus to the spermatheca (Edmonds *et al.* 2011) were also described. Here we report extensive roles for two classes of gap junction channels in mediating essential soma–germline interactions. Gap junctions composed of INX-8 and INX-9 in the soma and INX-14 and INX-21 in the germ line (referred to as INX-8/INX-9:INX-14/INX-21 channels) have a profound effect on the proliferation of germline stem cells. Genetic epistasis experiments establish a role for INX-8/INX-9:INX-14/INX-21 channels that is independent of the GLP-1/Notch pathway. Unlike GLP-1/Notch signaling, INX-8/INX-9:INX-14/INX-21 channels are required for entry into the meiotic pathway of development and gametogenesis. Using DTC-specific expression experiments to rescue germline proliferation, we show that INX-8/INX-9:INX-14/INX-21 channels may also be required later for the viability of early embryos. By contrast, INX-8/INX-9:INX-14/INX-22 channels are required for the negative regulation of oocyte meiotic maturation. This analysis reveals gap junctions as a central defining feature of many soma–germline interactions in *C. elegans*.

Materials and Methods

Strains and genetics

The following strains were used: AU98 *inx-14(ag17) I*; BS553 *fog-2(oz40) V*; BS913 *unc-32(e189) glp-1(oz112)/ unc-36(e251) glp-1(q175) III*; BS3392 *gld-2(q497) gld-1(q485)/hT2[dpy-18(h662)] I*; *unc-32(e189) glp-1(q175)/ hT2[bli-4(e937)] III*; CB151 *unc-3(e151)*; CB3775 *dpy-20(e2017) IV*; DG2157 *inx-14(tm2865)/hT2(qIs48) I*; DG3614 *inx-8(tn1474) inx-9(ok1502) IV*; *tnEx195[inx-8(+) inx-9(+)*; *sur-5*::*gfp]*; DG3620 *sem-3(n1655) inx-9(ok1502) IV*; DG3621 *dpy-20(e1282)/sem-3(n1655) inx-8(tn1474) inx-9(ok1502) mIs11 IV*; DG3670 *inx-8(tn1474) inx-9(ok1502) IV*; *tnEx201[lag-2p*::*inx-8*::*gfp*; *myo-2p*::*TdTomato]*; *tnEx203[lim-7p*::*inx-8*::*gfp*; *str-1*::*gfp]*; DG3742 *sem-3(n1655) inx-8(tn1513) inx-9(ok1502)/ mIs11 IV*; DG3828 *inx-22(tm1661) inx-21(tn1522)/ hT2(qIs48) I*; DG3829 *inx-22(tm1661) inx-21(tn1523)/ hT2(qIs48) I*; DG3830 *inx-21(tn1524)/hT2(qIs48) I*; DG3831 *inx-21(tn1525)/hT2(qIs48) I*; DG3846 *inx-8(tn1474) inx-9(ok1502)/mIs11 IV*; DG3887 *inx-21(tn1540)/hT2(qIs48) I*; DG3888 *inx-21(tn1540)/hT2(qIs48) I*; *neIs5[Y43B11*::*pgl-1*::*gfp*; *rol-6(su1006)]*; *tnEx204[inx-8p*::*mCherry*; *str-1*::*gfp]*; DG3907 *inx-8(tn1474) inx-9(ok1502)/mIs11 IV*; *tnEx205 [lag-2p*::*inx-8*::*gfp*; *str-1*::*gfp]*; DG3908 *sem-3(n1655) inx-8 (tn1513) inx-9(ok1502) IV*; *tnEx206[inx-8*::*gfp*; *str-1*::*gfp]*; DG3909 *mIs11 IV*; *tnEx207[inx-8p*::*mCherry]*; DG3910 *sem-3(n1655) inx-8(tn1474) inx-9(ok1502) IV*; *tnEx208[str-1*::*gfp*; *inx-9*::*gfp]*; DG3911 *unc-119(ed3) III*; *tnIs103[inx-8*::*gfp*; *unc-119(+)]*; DG3912 *unc-119(ed3) III*; *tnIs104[inx-14*:: *gfp*; *unc-119(+)]*; DG3915 *sem-3(n1655) inx-8(tn1474) inx-9(ok1502)/mIs11 IV*; *neIs5[Y43B11*::*pgl-1*::*gfp*; *rol-6(su1006)]*; DG3916 *sem-3(n1655) inx-8(tn1474) inx-9(ok1502)/mIs11 IV*; *neIs5[Y43B11*::*pgl-1*::*gfp*; *rol-6(su1006)]*; *tnEx204[inx-8p*::*mCherry*; *str-1*::*gfp]*; DG3917 *inx-8(tn1474) inx-9(ok1502)/mIs11 IV*; *fog-2(oz40) V*; *tnEx205[lag-2p*::*inx-8*::*gfp*; *str-1*::*gfp]*; *FX3403 inx-21(tm3403) I*; FX4316 *inx-21(tm4316) I*; FX4591 *inx-21(tm4316) I*; *JK633 unc-36(e873)/ unc-32(e189) glp-1(q46) III*; JK2049 *qIs19[lag-2*::*gfp*; *rol-6(su1006)] V*; MT3858 *sem-3(n1655) IV*; *PD4792 mIs11 IV*; SA250 *tjIs54[pie-1p*::*GFP*::*tbb-2*; *pie-1p*::*2xmCherry*::*tbg-1*; *unc-119(+)]*; *tjIs57[pie-1p*::*mCherry*::*his-48*; *unc-119(+)]*; VC116 *inx-8(gk42) IV*; VC994 *inx-9(ok1502) IV*; *WM107 pgl-1(bn101) IV*; *neIs5[Y43B11*::*pgl-1*::*gfp*; *rol-6(su1006)]*; XA774 *gna-2(qa705) unc-55(e1170)/gld-1(q485)*; and XM1011 *inx-22(tm1661) I*.

Strain constructions followed standard genetic procedures. For strains with extrachromosomal arrays, typically at least three independent lines were obtained; where no differences between lines were noted, one line was chosen as representative and provided in the strain list.

To isolate *inx-8 inx-9* double mutants, *sem-3 inx-9* males were mutagenized with EMS and crossed to *dpy-20* hermaphrodites. The *inx-8 inx-9* locus lies ~20 kb from *dpy-20*. Approximately 4200 hermaphrodite cross-progeny were individually plated, and broods were examined for the absence of the Sem-3 class (*i.e.*, bag of worms phenotype). Candidate *sem-3 inx-9* sterile mutants were examined for phenotypic resemblance to *inx-14(tm2864)* (few germ cells produced) and further characterized. The *sem-3(n1655)* mutation was removed from the *inx-8(tn1474) inx-9(ok1502)* genetic background by recombination, and we observed no change in the severity of *inx-8(tn1474) inx-9(ok1502)* germline phenotypes.

To follow germ cell divisions in live L1-stage animals, we made use of *unc-3(e151)* to reduce movement on agar pads. Germ cell division appeared unaffected in *e151* animals, and germ cell counts in 13 gonad arms of early L2 *e151* animals averaged 6.6 ± 2 (range 4–11). A strain of genotype *inx-8(tn1474) inx-9(ok1502)/ mIs11 IV*; *unc-3(e151) X* was used to identify *inx-8 inx-9*; *unc-3* homozygous mutant L1s. After germ cell divisions were followed during mid-late L1 stage,

animals were re-examined the following morning to ensure that somatic gonad cells Z1 and Z4 and their descendants had divided and to score germ cell divisions.

For genetic mosaic analysis of *inx-8(+) inx-9(+)* using DG3614, we did not formally screen for losses of the rescuing array in the germline lineage. However, during the course of strain maintenance, we identified several *sur-5*::*gfp(+)* animals that were fertile but produced only sterile progeny, suggesting, as expected, that *inx-8(+) inx-9(+)* function is not required in the germ line.

Electron microscopy

Freeze-fracture replicas were prepared as described (Hall *et al.* 1999), with the exception that samples were cryoprotected in 25% glycerol overnight prior to freezing. Specimens were examined by transmission electron microscopy (TEM) using an FEI Tecnai G2 Spirit BioTWIN electron microscope at a high-tension setting of 80 kV. The distal–proximal axis of the gonad was ascertained by the relative size of germ cells. We examined sheath:germ cell gap junctions in >40 distal gonad arms, but no specimens contained a clearly recognizable distal tip cell.

TEM methods were as explained by Hall (1995). Microscopy used Phillips EM300 and CM10 instruments. All imaging was collected on 4489 film (Eastman Kodak Co., Rochester, NY) and then digitized.

Antibody production

Maltose-binding protein fusions with the respective carboxyl termini of INX-8 (99 amino acid residues) and INX-21 (168 amino acid residues) were used to immunize rabbits, guinea pigs, or rats (Cocalico Biologicals, Inc., Reamstown, PA; Pocono Rabbit Farm and Lab, Canadensis, PA). Antibodies were affinity-purified using corresponding glutathione-*S*-transferase fusion proteins. Isolation of anti-INX-14 and anti-INX-22 has been previously described (Govindan *et al.* 2009). Affinity-purified anti-INX-8 was shown to cross-react with INX-9 since it detected a signal in *inx-8(gk42)* and *inx-9(ok1502)* single mutants, as well as *inx-8(tn1474) inx-9(ok1502)* mutants rescued by either *inx-8*::*gfp* or *inx-9*::*gfp*. Because *inx-8 inx-9* double mutants are sterile and produce few germ cells, the specificity of the anti-INX-8 antibody could be confirmed by staining double-mutant progeny rescued for germline proliferation by DTC expression (from strain DG3907) and observing an absence of staining in the proximal gonad. As described in *Results*, anti-INX-21 appears to detect INX-21 based on its unique expression profile in comparison to other germline innexins. The staining patterns in the wild type and *inx-22(tm1661)* mutants appear indistinguishable. However, we cannot exclude the possibility of some cross-reactivity with INX-22.

Immunocytochemistry

A Zeiss motorized Axioplan 2 microscope with a 63× PlanApo (numerical aperture 1.4) objective lens was employed for fluorescence microscopy. Images were acquired with an AxioCam MRm camera and AxioVision acquisition software. Some images were acquired using an apotome adaptor (Zeiss), as indicated.

Anti-INX antibodies, anti-GFP monoclonal antibody 3E6, and anti-phospho-H3 (Ser10; Millipore) antibodies were used to stain dissected gonads (fixed in 3% formaldehyde in MRWB buffer for 1.25 hr, followed by a 20-min incubation in 10 mM DTT in Tris–Triton buffer; Finney and Ruvkun 1990), or whole-animal mounts (fixed in 1% formaldehyde for 1.5 hr; Finney and Ruvkun 1990). Fixed specimens were blocked overnight (5% BSA, 1× PBS, 0.5% Tween-20, 0.02% sodium azide) and stained with the appropriate primary or secondary antibodies in the same solution. Anti-dpMPK-1 staining followed Lee *et al.* (2007).

DAPI staining of live embryos was carried out by dissecting gravid adults in a 0.25μg/ml DAPI solution. Embryos released by dissection were incubated for ~10 min, washed twice, and mounted for examination.

Transgene constructs

Details and sequences of constructs are available upon request. In overview, *inx-8 inx-9* mutants were rescued with a 9-kb *Bam*HI genomic DNA fragment isolated from cosmid clone ZK792. This fragment includes ~3 kb of sequence upstream of the predicted translational start site for *inx-8* and 0.7 kb downstream of the polyadenylation signal for *inx-9*. A rescuing *inx-8*::*gfp* C-terminal fusion construct includes 3 kb of this fragment upstream of *inx-8* but no *inx-9* sequences. A rescuing *inx-9*::*gfp* C-terminal fusion construct includes 3 kb upstream of the *inx-8* translational start site plus sequences representing the first 38 amino acid residues of INX-8; the remainder of the *inx-8* coding region was deleted. All *inx-8* and *inx-9* constructs were microinjected for transformation rescue at 2 ng/μl. A partially rescuing *inx-14*::*gfp* C-terminal fusion construct is derived from an 8.1-kb *Pst*I genomic fragment isolated from cosmid clone F07A5 that includes 4.4 kb upstream of the predicted *inx-14* translational start site. Integrated forms of *inx-8*::*gfp* and *inx-14*::*gfp* were isolated by biolistic transformation of *unc-119* animals.

lag-2p::*inx-8*::*gfp* was constructed by cloning a 3.2-kb *Sal*I fragment from pGC389 (gift from J. Hubbard), which lies ~170 bp upstream of the predicted *lag-2* translational start site, into *inx-8*::*gfp* at a position 45 bp upstream of the first exon.

inx-8p::*mCherry* includes insertion of mCherry sequences into the first exon of *inx-8* 16 bp upstream of the *inx-8* translational start site. Sufficient *inx-8* and *inx-9* sequences have been removed such that neither gene can be expressed in this construct.

inx-8p::*str-1*::*gfp* was made by PCR amplification of *str-1* sequences from fosmid clone WRM068aB11, followed by replacement of *inx-8* sequences with *str-1* in an *inx-8*::*gfp*-expressing construct.

lim-7p::*inx-8*::*gfp* includes 1.1 kb of the first intron of *lim-7*, including a 45-bp enhancer identified as being necessary and sufficient for sheath expression (Voutev *et al.* 2009), positioned

45 bp upstream of the first exon of an *inx-8*::*gfp* construct. No other potential *inx-8* promoter sequences are included.

Isolation of inx-21 deletions using CRISPR-Cas9 genome editing

To target specific sites in *inx-21* for Cas9 scission with single-guide RNA (sgRNA), primers *U6prom EcoRI F/inx-21g1R* and *inx-21g1F/U6prom HindIII R* or *U6prom EcoRI F/inx-21g2R* and *inx-21g2F/U6prom HindIII R* were used to generate overlapping PCR products that could be amplified and used to replace the *Eco*RI/*Hin*dIII insert in pU6::*unc-119*sgRNA to generate pU6::*inx-21*sgRNA1 and pU6::*inx-21*sgRNA2, following Friedland *et al.* (2013). Typically for microinjection transformation, *inx-21* sgRNA constructs were co-injected at 100 ng/μl each, along with P*eft-3*::Cas9-SV40 NLS::*tbb-2* 3′ UTR at 100–150 ng/μl and a *myo-2p*::*TdTomato* marker at 2–4 ng/μl. A repair template (also injected at 100 ng/μl) used to isolate *inx-21(tn1540)* was made by cloning the *C. briggsae unc-119* gene, obtained from pGC90, between 1-kb *inx-21* DNA sequence blocks flanking either side of the targeted deletion, isolated by PCR using primers F7487Xba with R8572Pst and F14283Pst with R15347Xho.

Primer sequences used were the following: *inx-21g1F*—5′-GATTCGATAAATCCACTCAAGTTTTAGAGCTAGAAATAGCAAGTTA-3′; *inx-21g1R*—5′-TTGAGTGGATTTATCGAATCAAACATTTAGATTTGCAATTCAATTATATAG-3′; *inx-21g2F*—5′-GATGATGTCCGAATCTGATGGTTTTAGAGCTAGAAATAGCAAGTTA-3′; *inx-21g2R*—5′-CATCAGATTCGGACATCATCAAACATTTAGATTTGCAATTCAATTATATAG-3′; F7487Xba—5′-AAAATCTAGACGTCAAATATGGTGCGCAATACGC-3′; R8572Pst—5′-AAAACTGCAGACAAGAAGAATCGGAACCAGTGG-3′; F14283Pst—5′-AAAACTGCAGATGAGGAACCAATGATCAGTCCAGC-3′; R15347Xho—5′-AAAACTCGAGTTGCGATACTGGATTGGAGAGCGAC-3′; other primer sequences are available on request.

Results

Freeze-fracture TEM reveals formation of gap junctions between germ cells and sheath cells in the distal gonad arm

Previously, we reported that the *C. elegans* germ cell gap junction proteins INX-14 and INX-22 colocalize throughout the adult gonad (Govindan *et al.* 2009). Gap junctions forming between developing oocytes and the somatic sheath cells in the proximal gonad arm have been described (Hall *et al.* 1999). Gap junctions in the distal gonad arm were not seen by standard TEM methods, making the detection by immunofluorescence of presumptive gap junctions in this location somewhat surprising. The immunofluorescent signals for INX-14 and INX-22 appeared as fine puncta in the distal gonad but large puncta in the proximal gonad. These puncta likely represent aggregates of individual gap junction channels. Thus, it was possible that distal gap junctions might be small in comparison to those in the proximal arm and not observable by TEM. In an attempt to corroborate immunofluorescence results with electron microscopy evidence, TEM analysis of freeze-fracture samples was used to search for gap junctions in the distal arm.

Distal gonad arms could be recognized in freeze-fracture specimens by the appearance of tightly packed hexagons or rhomboids, each of which represented a germ cell (Figure 2A). A ridge resulting from a thin wedge of somatic sheath dipping down between germ cells was often observed (Figure 2, B–D). Fractures are thought to most commonly occur between the two leaflets of the lipid bilayer of one cell membrane (Rash and Hudson 1979). These fractures may reveal features associated with an E-face (in Figure 2, representing the outer membrane leaflet of the somatic sheath cell overlying the germ cell) or P-face (representing the inner membrane leaflet of the germ cell). Historically, freeze-fracture analyses of gap junctions have revealed large, tightly packed clusters of particles that are larger than most other membrane particles, ~8–10 nm for connexins (*e.g.*, Goodenough and Revel 1970) and 12–13 nm for innexins (Flower 1972, 1977). However, aggregates of more loosely arranged innexin or connexin particles in apparent mature gap junctions, or at sites of nascent gap junction assembly (formation plaques), have also been described (Baerwald 1975; Swales and Lane 1985; Johnson *et al.* 2012). Previous freeze-fracture studies on *C. elegans* have shown that plaques of pits and particles show a tissue-specific range of sizes and leaflet distribution, but tend to be small (Hall 1992).

Several dozen distal gonad arms were identified in freeze-fracture samples and examined for evidence of gap junction formation between germ cells and somatic sheath cells. Large gap junctions of the type seen in the proximal arm were not evident. Most commonly, we found examples of small clusters of loosely aggregated membrane particles associated with the P-face (Figure 2 and Supporting Information, Figure S1). Clusters of corresponding "pits" could be identified on the E-face of the sheath (Figure 2, D–F). Pits often occur on one fracture face of gap junctions because of the strong association between hemichannels on apposing cells. Although most of the large particles were anchored with the P-face, a small percentage remained associated with the E-face in the neighborhood of pits (Figure 2, D–I). Evidence that these particles and pits reflect similar molecules was seen where a fracture jumped from one face to another within a cluster of P-face particles and a mixture of E-face pits and particles (Figure 2, G–I). These particles were also seen as widely scattered individual particles and occasionally as large clusters of many dozens. Rarely, a long extensive field of pits could be detected (Figure S1).

Consistent with previous reports of innexin freeze-fracture particles (Flower 1972, 1977), the size of these particles averaged ~13.5 nm (13.5 ± 1.6 nm, $n = 63$, for particles measured on the E-face of the sheath; 13.3 ± 1.8 nm, $n = 76$, for particles measured on the P-face of germ cells; and 13.9 ± 1.7 nm, $n = 57$, for center-to-center channel spacing of closest E-face pits). Therefore, based on particle size, the appearance of a mixture of pits and particles on the same fracture face, and

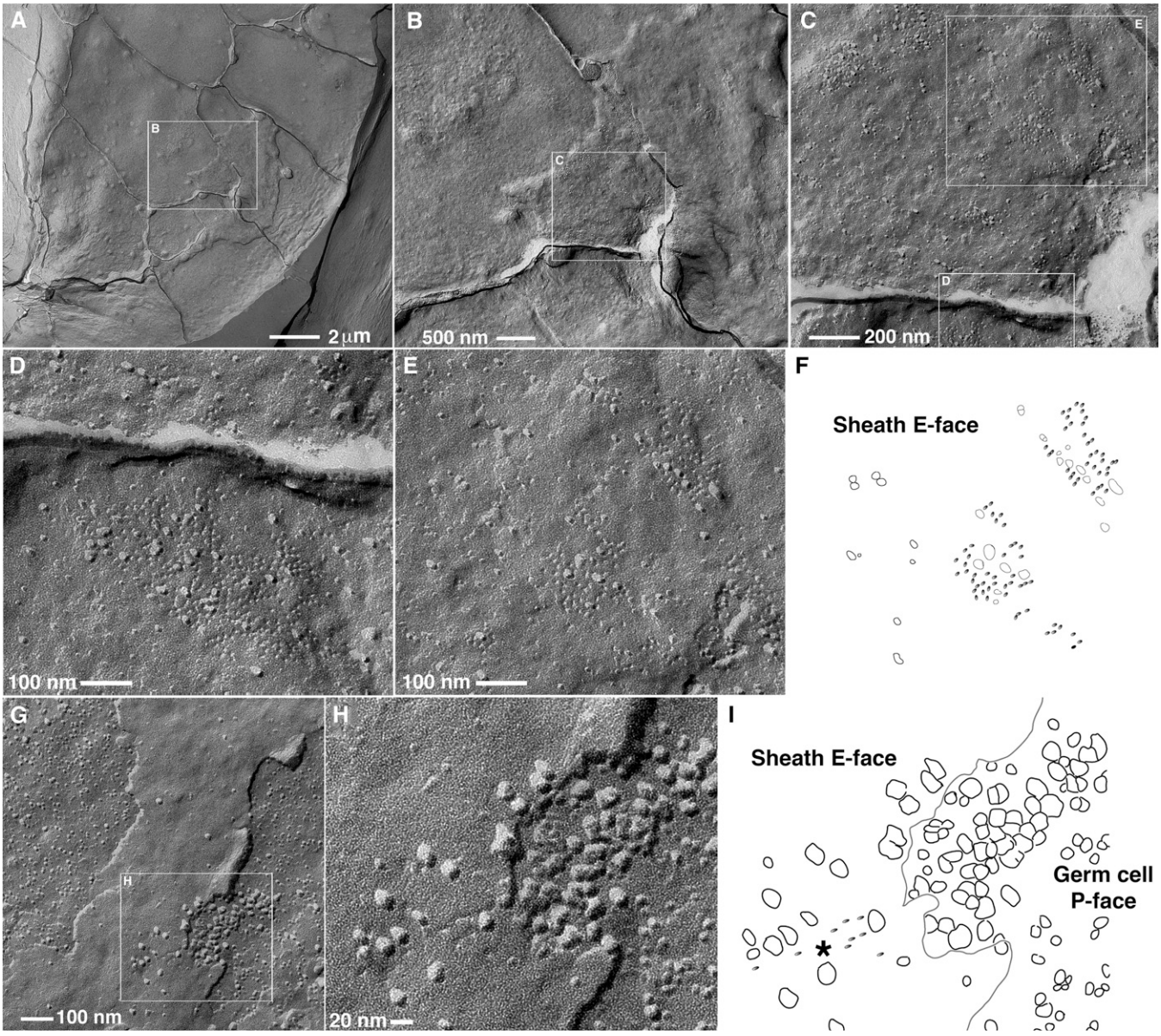

Figure 2 Freeze-fracture EM analysis reveals gap junction-like particles in the distal gonad. (A–F) Increasing magnification of a region of germ cells in the distal arm. Boundaries between germ cells are easily distinguished in A and B; in C and D, a raised ridge of sheath inserting between germ cells is apparent, and loosely packed clusters of pits, with a few large particles scattered among them on the exposed E-face of the sheath, are most commonly found near cell boundaries. (E) Higher magnification of the inset region in C; (F) Diagram of pits (small dark ovals) and particles (open shapes) seen in E. (G–I) Cross-fracture in a presumptive gap junction in the distal gonad. (H) Higher magnification of inset in G shows a cluster of large particles evident on the germ cell P-face; where the fracture plane jumps to the sheath E-face, a mixture of several pits and large particles are seen (asterisk in I). (I) Diagram of pits (small dark ovals) and particles (open shapes) seen in H; line indicates approximate position of the fracture changing faces. Bar values are indicated.

the resemblance of the distribution of particle aggregates to previous immunofluorescence results for INX-14 and INX-22 (Govindan *et al.* 2009), we conclude that these particles represent innexin gap junction molecules.

INX-8, -9, -14, -21, and -22 colocalize throughout the gonad

Prior work established germline functions for *inx-14* and *inx-22* as negative regulators of meiotic maturation (Govindan *et al.* 2006, 2009; Whitten and Miller 2007) and a role for *inx-14* in germline proliferation (Govindan *et al.* 2009). If these genes indeed encode germ cell components of gap junctions, we would expect that other innexin genes may encode corresponding somatic gap junction components that contribute to the same biological processes. The innexin genes *inx-8* and *inx-9* represent a recent gene duplication (only a single innexin resides at this locus in *C. briggsae*). Based on corresponding GFP fusions expressed in gonadal sheath cells, especially the proximal sheath (Starich *et al.* 2001), *inx-8* and *inx-9* were candidates for encoding somatic

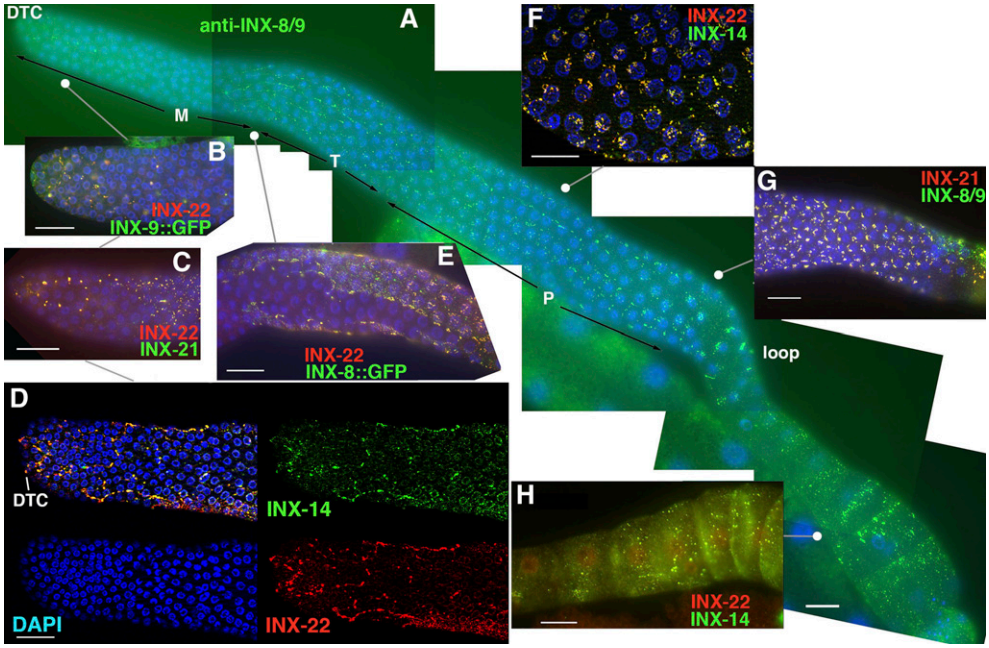

Figure 3 Co-expression of innexin proteins in the adult gonad. (A) Antibodies specific to the carboxyl termini of INX-8 and closely related INX-9 detect expression in the DTC and somatic sheath cells, as seen in a composite of a dissected gonad arm. Expression is absent or much reduced in the mitotic zone (M) and in areas where no somatic cell overlies the germ line. (B–H) Colocalization of innexins throughout the gonad. In B–H, the approximate corresponding position in the gonad arm is compared to A. (B–D) Colocalization in the region of the DTC of INX-9::GFP and INX-22 (B), INX-21 and INX-22 (C), and INX-14 and INX-22 (D). A medial focal plane of a dissected gonad (D) shows that INX-14 and INX-22 appear to associate with DTC processes that intercalate between germ cells. (E) INX-8::GFP and INX-22 colocalization in the region of the distal end of sheath coverage over germ cells. (F) INX-14 and INX-22 colocalization among pachytene-stage germ cells. (G) INX-8/9 and INX-21 colocalization in the loop region where germ cells leave the pachytene stage. (H) INX-14 and INX-22 colocalize in the proximal arm. M, mitotic region; T, transition zone; P, pachytene. Images in D and F were taken using an apotome adaptor. Bars, 20 μm.

hemichannels that might dock with hemichannels in the germ line. *inx-21* is SL2-transpliced and resides downstream in an operon with *inx-22*, and thus both innexins might be co-expressed and contribute to gap junctions in the gonad (Land *et al.* 1994; Blumenthal 2012). Antibodies generated against the carboxyl termini of INX-8, INX-14, INX-21, and INX-22 were used to investigate their respective expression patterns. INX-8 and INX-9 share 73% identity in the carboxyl termini (83% sequence identity overall), and antibodies raised against INX-8 were shown to cross-react with INX-9 (see *Materials and Methods*). We refer to this antibody signal as INX-8/9. INX-8::GFP and INX-9::GFP fusion protein constructs were used to evaluate the corresponding individual expression patterns.

Expression of INX-8, -9, -14, -21, and -22 overlapped closely throughout the gonad in wild-type adult hermaphrodites (Figure 3). In distal arms (Figure 3, A–G), clusters of fine puncta were associated with each germ cell, as previously reported for INX-14 and INX-22 expression (Govindan *et al.* 2009). INX-8/9, INX-8::GFP, and INX-9::GFP were expressed in the DTC in addition to the somatic sheath (Figure 3, A and B). In the DTC, INX-8/9, INX-8::GFP, and INX-9::GFP associated with long processes that extended from the DTC proximally, especially those running between germ cells and intercalating among them. INX-14, -21, and -22 colocalized to puncta associated with these processes (Figure 3, B–D). At the distal limit of sheath cell coverage of germ cells, longer formations sometimes appeared associated with the apparent edge of the sheath cells (Figure 3, A and E). At the loop region of the gonad arm, individual puncta appeared in larger, higher-density aggregates (Figure 3, A and G). In the proximal arm, puncta size was more variable, with many appearing to be considerably larger than the fine puncta seen in the distal arm (Figure 3, A and H). Although all innexins appeared to colocalize, INX-21 differed from the other innexins in that its expression level was relatively higher in the distal gonad compared to the proximal gonad (Figure 4). In contrast, the expression levels of INX-8, INX-9, INX-14, and INX-22 appeared higher in the proximal gonad (Figure 3A and Figure 4). Throughout the gonad the localization patterns of INX-8::GFP and INX-9::GFP were indistinguishable.

In addition to gonadal expression, antibody staining of whole mounts suggested that INX-8/9 may be expressed in some pharyngeal and a few other head neurons (T. Starich, unpublished results), but because the antibody reacted primarily with processes and not cell bodies, we did not attempt to identify these neurons. Expression driven by the *inx-8* promoter in a small set of neurons has previously been described (Altun *et al.* 2009).

Male gonads were examined and found to express INX-8, -9, -14, -21, and -22 as well (Figure S2). Presumptive gap junctions forming between both male distal tip cells and germ cells were detected with antibodies specific to INX-8/9, INX-14, INX-21, and INX-22 (Figure S2, A–C). Both INX-8::GFP and INX-9::GFP were expressed in the DTCs. No expression was detected in the transition zone, but innexin expression appeared to outline individual germ cells in the pachytene region (Figure S2, A and C). All five innexins are also expressed in the regions occupied by differentiated spermatocytes and sperm, with evidence of puncta formation. Expression of INX-9::GFP visualized somatic coverage of spermatids, probably by cells of the seminal vesicle (Figure S2D), but somatic coverage of germ cells in the pachytene region of the male gonad has not been described.

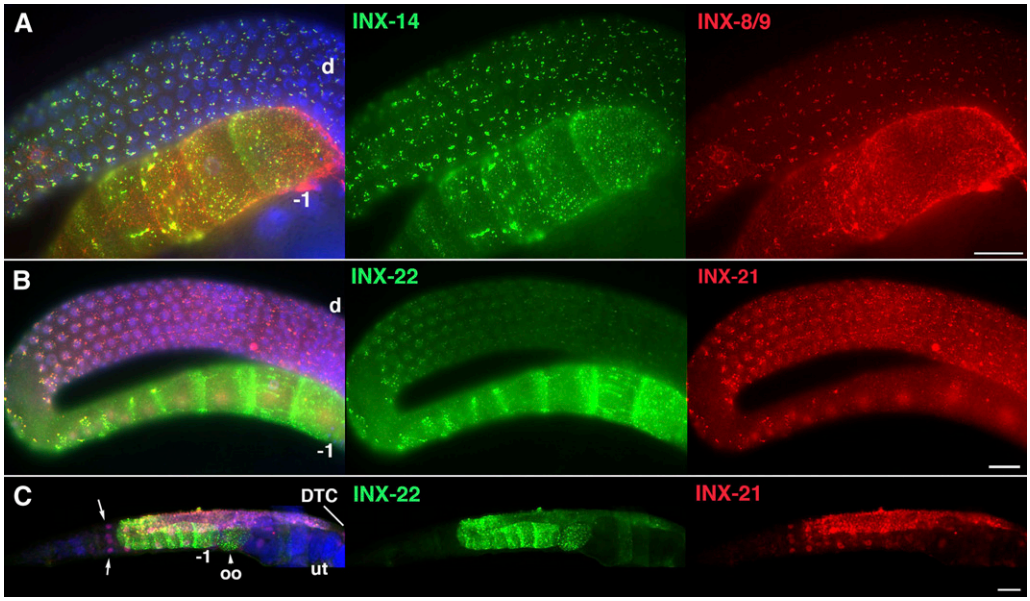

Figure 4 Relative distribution of innexins along the distal–proximal axis. (A) INX-8/9 and INX-14 accumulate to higher levels in the proximal gonad arm. (B and C) INX-22 and INX-21 differ in their relative distributions, with INX-22 exhibiting higher expression levels proximally, whereas INX-21 is enriched distally. A dissected gonad (B) and a whole mount (C) are shown. Arrows in C indicate nuclei outside the gonad showing anti-INX-21 background staining. d, distal arm; –1, most proximal oocyte; ut uterus; oo, ovulated oocyte. Bars, 20 μm.

Innexins are expressed in the primordial gonad

Identification of gap junctions in adult gonads raised the question of when soma–germline gap junctions are first established. Examination of earlier developmental stages showed that all five innexins are expressed in the primordial gonad (Figure 5), consisting of somatic gonadal precursors Z1 and Z4 and the primordial germ cells Z2 and Z3. In a few serendipitous cases, expression of INX-22 was detected prior to hatching in pretzel-stage embryos (Figure 5A). Early larval expression patterns differ from adults in that distinct, well-defined puncta potentially corresponding to gap junctions are less clearly discernible. In L2–L4 larval stages (Figure 5, G–I), germ cell innexins appear to be continually expressed, and somatic innexins are expressed predominantly in the DTC. In late L2 and early L3 stages, as the gonad arm lengthens, the migrating DTC seems to trail a process behind it that maintains contact with the germ cell compartment (Figure 5G). The DTC appears to form gap junctions with germ cells at both long external processes and processes that intercalate between germ cells (Figure S3). At this time, a second, more proximal focus of somatic innexin expression was sometimes detected. Although this second focus might represent extensions from the DTC, expression of *inx-9*::*gfp* suggested that other somatic cells in addition to the DTC might be involved (Figure 5G and Figure S3). By the late L3 stage, the DTC no longer appears to be in contact with all of the germ cells (Figure 5, H and I). To better understand the contacts between germ cells and the DTC, we examined early L4-stage animals by TEM (Figure 6). We observed several processes trailing behind the DTC cell body on the outer edge of the germline, as well as extensions that dig deeply between germ cells (Figure 6). The immunofluorescence results suggest that gap junctions form between the DTC and germ cells at both the outer and the inner DTC arms (Figure 3, B–D; Figure 6D).

The *inx-8* promoter was fused to mCherry, and *inx-8p*::*mCherry* was expressed during larval development in most or all of the somatic gonad cells derived from Z1 and Z4, including the DTC, sheath/spermathecal precursors, and uterine cell precursors (Figure 5, J–L). We conclude that, although expression of INX-8/9 appears to be strongest in the DTC during larval development, other somatic gonad cells may also express INX-8/9 at this time.

Innexins are interdependent for their localization

Colocalization results suggested that somatic INX-8 and -9 associate in gap junction channels with INX-14, -21, and -22. The dependence of individual innexin localization on other innexins was examined in mutant or RNA interference (RNAi)-mediated knockdown backgrounds (Figure 7 and Figure S4). *inx-14(tm2684)* mutants produce few germ cells (average 27 ± 7 per gonad arm, range 12–43, $n = 20$) that often become necrotic in adults (75%, $n = 40$), making them unsuitable for antibody staining. INX-14 levels were reduced by microinjection of *inx-14* double-stranded RNA (dsRNA). Some progeny were as severely affected as *inx-14(tm2864)* mutants and were unsuitable for gonad dissection; however, the gonad arms of some sister progeny that produced oocytes were examined, and it was found in these animals that INX-22 failed to localize to presumptive gap junction puncta (Figure 7, A–C). These results suggest that INX-14 is required for INX-22 to localize properly. In animals in which INX-14 levels are diminished but not completely eliminated by *inx-14(RNAi)* treatment, it appears that a sufficient number of INX-14-containing channels must be expressed to rescue oogenesis but not to aggregate into puncta detectable by immunofluorescence.

As a second way of evaluating the localization dependence of other innexins on INX-14, we examined the hypomorphic *inx-14(ag17)* allele. The *inx-14(ag17)* allele is an R326H

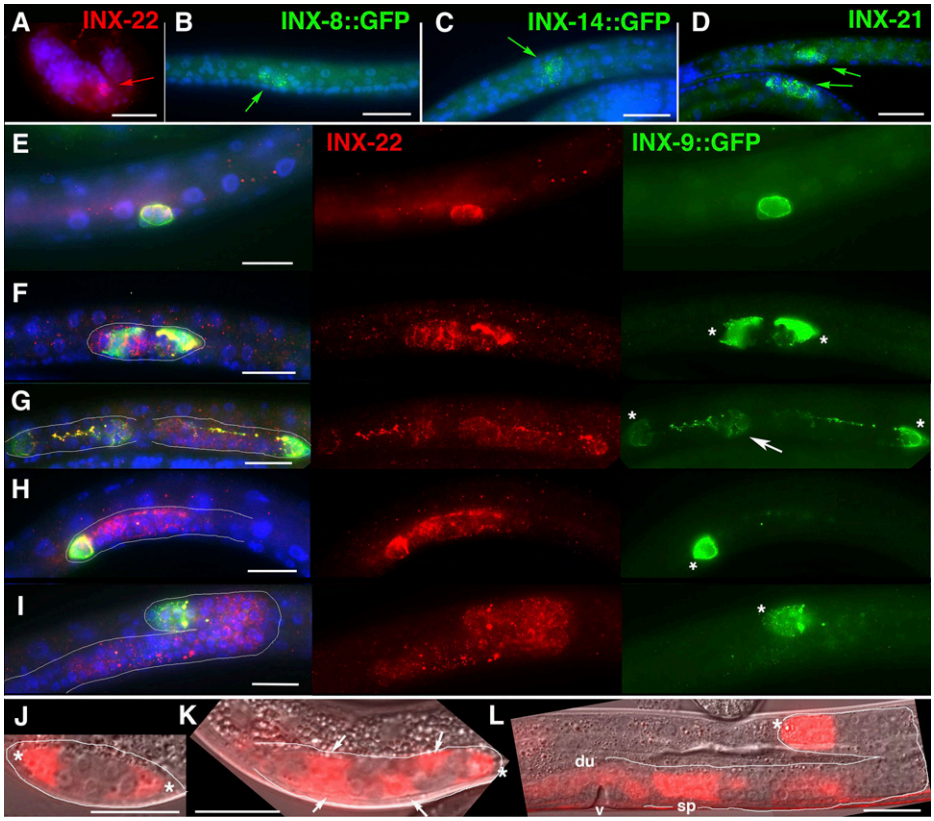

Figure 5 Developmental expression of gonadal innexins. Whole mounts were stained with innexin-specific antibodies or anti-GFP where appropriate. (A) INX-22 expressed in the primordial gonad in a late-stage embryo. (B) INX-8::GFP expression in first larval stage (L1) animal. (C) INX-14::GFP expression in an L1 animal. (D) INX-21 in earlier (upper) and later (lower) L1 stage animals. (E–I) INX-9::GFP and INX-22 co-expression during larval development. (E) L1 stage. (F) Late L1/early L2 stage (asterisks indicate positions of distal tip cells). (G) L2 stage (arrow indicates second focus of INX-9::GFP expression). (H) L3 stage. (I) Early L4 stage after DTC has migrated to the dorsal side. (J–L) Expression of *inx-8p*::*mCherry* in L1 (J; asterisks indicate position of Z1 and Z4), early L2 (K; asterisk indicates DTC, and arrows indicate other somatic cells expressing mCherry), and L4 (L; asterisk, DTC; sp, spermatheca; du, dorsal uterus; v, developing vulva). Bars, 20 μm.

missense mutation in the predicted intracellular carboxyl terminus near the fourth transmembrane (TM) domain (Miyata *et al.* 2008; this study). *inx-14(ag17)* animals are resistant to bacterial pathogens and give reduced brood sizes at 25° (Miyata *et al.* 2008). The distribution of INX-8/9, INX-21, and INX-22 was greatly affected in *ag17* animals, being mostly diffuse, or, in the case of INX-8/9, sometimes found in concentrations where the sheath surrounds underlying germ cells (Figure 7, D and E; see Figure 3 and Figure 4 for the wild-type innexin distribution). INX-21 and INX-22 did not colocalize with INX-8/9 in these concentrations. We conclude that disruption of INX-14 expression affects the localization of germ cell INX-21 and INX-22 as well as somatic INX-8/9. Interestingly, in *inx-14(ag17)* mutants, the sheath coverage of germ cells extended distally in the gonad arm such that it bordered the DTC (Figure 7D).

In *inx-22(tm1661)* mutants, which produce healthy broods, both INX-8 and INX-14 colocalized to puncta in the distal arm but not in the proximal arm (Figure 7F). INX-21 localization was not greatly affected (Figure 7G). In *inx-21(ok2524)* and *inx-21(tm4316)* mutants, INX-22 localization appeared only marginally affected (Figure S4); however, we show below that these are not null alleles of *inx-21*. The *inx-22* mutant results indicate that, in the proximal arm, INX-22 is required for the bulk of INX-14 and INX-8/9 localization, but, in the distal arm, the presence of INX-21 seems sufficient for INX-14 and INX-8/9 to localize to puncta.

Because of the sequence similarity between *inx-8* and *inx-9*, and because respective deletion mutants have no obvious phenotypes (*gk42* brood size average 214 ± 25; *ok1502* brood size average 210 ± 34, $n = 9$ for both), we presumed that these innexins likely overlap functionally. RNAi knockdown of *inx-8* in *inx-9(ok1502)* mutants was used to assess effects on localization of germ cell innexins. As with *inx-14*, *inx-8(RNAi)* in *inx-9(ok1502)* animals resulted in some progeny producing short gonad arms with few germ cells that were unsuitable for dissection, while some siblings that produced gonad arms with oocytes showed loss of INX-14, INX-21, and INX-22 localization throughout the gonad arm (Figure 7, H and I).

Together, these results (summarized in Figure S5) suggest that in germ cells the inability of INX-21 and INX-22 to localize to puncta in the absence of INX-14 reflects a requirement for INX-14 in the formation of all germline hemichannels. In the absence of INX-14, no functional germ cell hemichannels arise with which INX-8/9 somatic hemichannels can dock and form intercellular channels, and therefore INX-8/9 fails to localize into the aggregates of channels that are visualized as puncta by immunofluorescence. Conversely, INX-8 and INX-9 appear to be necessary for all germline hemichannels to localize. INX-21 expression in germ cells is sufficient for INX-14 to form functional hemichannels because in *inx-22(tm1661)* mutants INX-14 (as well as INX-8/9) localizes to presumptive gap junction puncta in the distal arm. INX-22 also appears to be sufficient to localize INX-14 because the bulk of proximal INX-14 expression is lost in *inx-22(tm1661)* mutants (Figure 7F). INX-21 and INX-22 puncta colocalize, and it is possible some germline hemichannels could contain

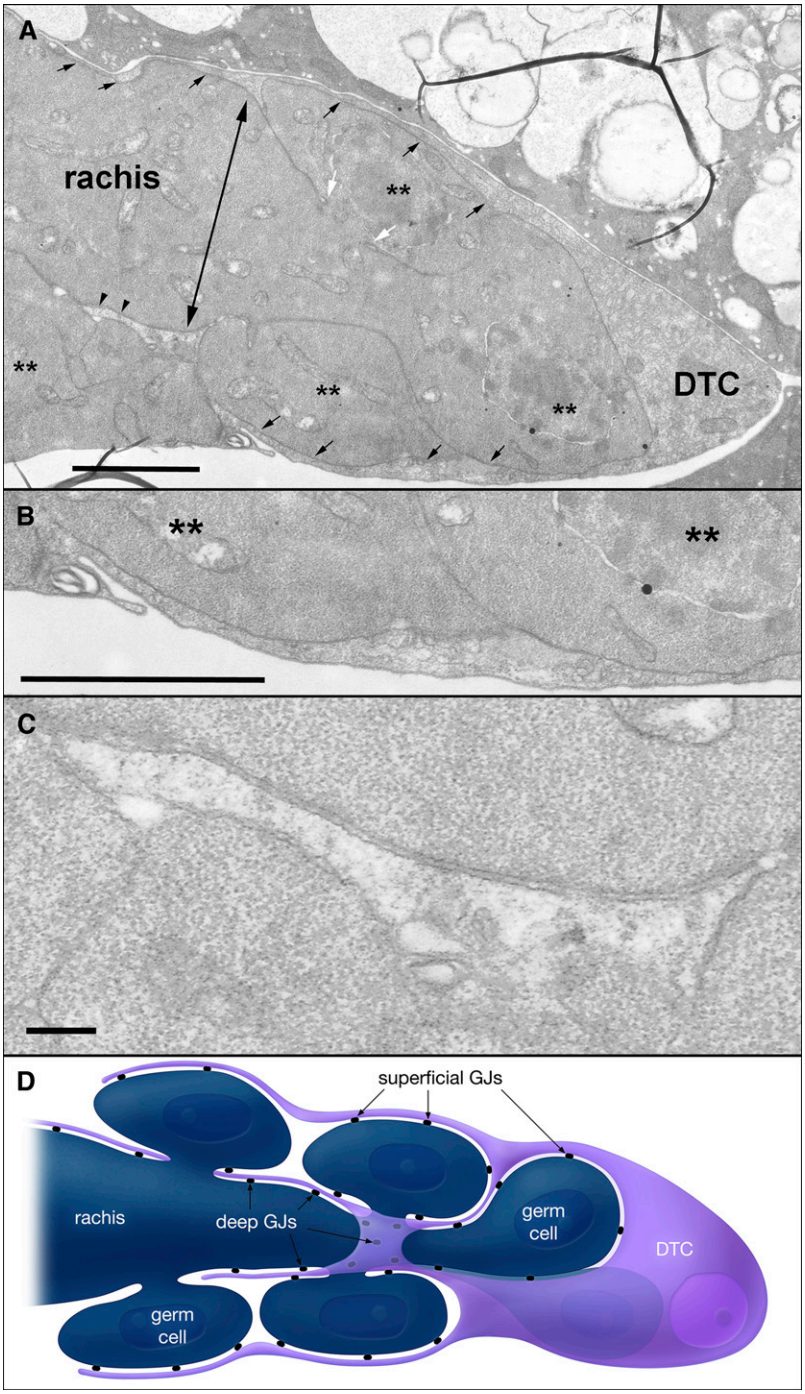

Figure 6 (A–D) Views of the DTC during outgrowth toward the dorsal midline in early L4 stage, viewed by TEM. A wild-type larva (L4 + 3 hr) was sectioned lengthwise to view the DTC during its migration, pulling the germ cells behind it. (A) The DTC is migrating rightward, with several arms (small arrows) seen trailing behind it (leftward) on the outer edge of the germ line, before digging deeper between germ cells at the double-headed arrow to squeeze and envelop only the most distal germ cells (double asterisks). The DTC soma lies at the very front of the gonad arm. It is possible that some gap junctions form between the DTC soma and the nearest germ cells, as they are in very close contact. Note that all germ cells are syncytial to the rachis (white arrows mark borders of one germ cell's cytoplasmic connection to rachis). Additional DTC arms trail leftward from the squeezing zone to run either along an outside route over the tops of germ cells (at top left) or along a deeper route (black arrowheads) close to the rachis. Bar, 1.0 μm. (B) A closer view of an outer DTC arm, running directly from the DTC soma over the tops of two germ cells (double asterisks), with their plasma membranes closely apposed over most of their length. Evidence from antibody staining suggests that many gap junctions form between such outer arms and the germ line, but they are never visible in thin sections due to their small size and/or loose channel packing (see Figure 2). Bar, 1.0 μm. (C) A closer view of an inner squeezing zone and a DTC arm extending along an inner route, close to the rachis and beneath the outer germ line layer. DTC cytoplasm is distinctly less electron-dense than the germline cytoplasm. The DTC and germ cell plasma membranes are closely apposed. Evidence from antibody staining suggests that the highest concentration of small gap junctions lies along these inner DTC arms, potentially contacting both the rachis and the germ cells. Bar, 0.1 μm. (D) Illustration summarizing the relations between the DTC and the germ line. The DTC (violet) is crawling to the right, with its nucleus near the leading edge. All germ cells are syncytial to the rachis via connecting cytoplasm (dark blue). The DTC completely envelops several leading germ cells; for clarity, only two cells are shown, with one being undraped to depict how the DTC surrounds and contacts the germ cell's outer surface. Trailing DTC processes emanate from the soma and connect to a narrow ring where the DTC squeezes the rachis. This tight squeezing may assure that the two tissues cannot be separated during DTC crawling. Additional thin DTC processes trail away from the ring to extend along two routes to either touch the outer edge of the germ cells or dive deeper to contact the rachis and/or the undersides of germ cells. Black dots indicate potential sites for DTC–germline gap junctions. Although the deeper arms seem to form the most junctions, we cannot be certain from present EM data whether they tend to contact the rachis or the underside of germ cells, or both.

both innexins. However, the relative expression level of INX-21 decreases going from the distal arm to the proximal arm, while that of INX-22 increases (Figure 4); therefore, a co-association of INX-21 and INX-22 in hemichannels is not the norm. We conclude that soma–germline gap junction channels are likely composed of INX-8/9 somatic hemichannels docked with germline hemichannels containing either INX-14/INX-21 or INX-14/INX-22.

Endocytosis of INX-8 and INX-9 by ovulating oocytes confirms soma–germline gap junction channel formation

Further evidence that somatic INX-8/9 physically interacts with germline innexins was seen in oocytes undergoing meiotic maturation and ovulation or early embryogenesis. Although INX-8/9 is expressed in the somatic sheath in the proximal gonad, the presence of INX-8::GFP in early embryos was often

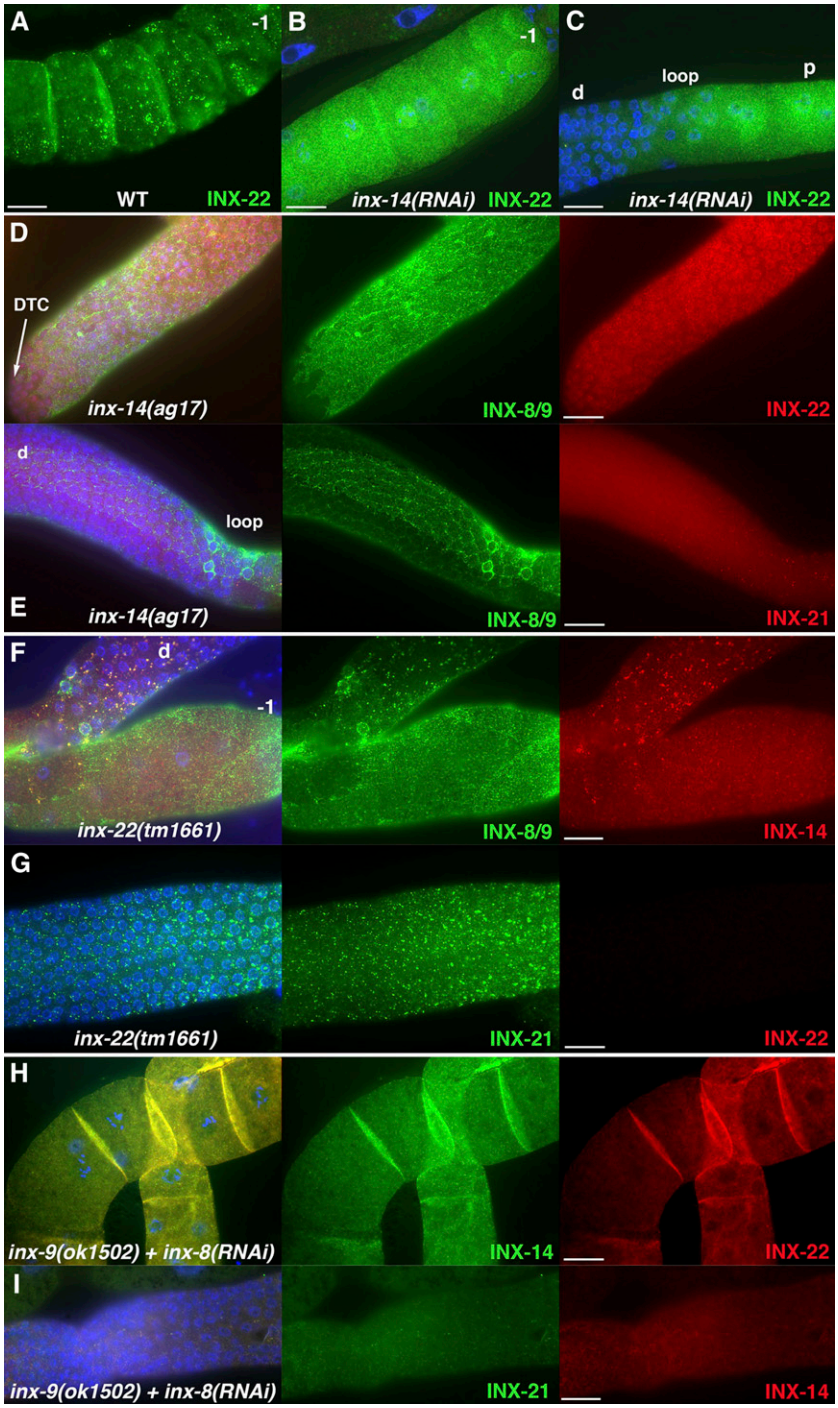

Figure 7 Gonadal innexins are interdependent for localization to presumptive gap junctions. (A) Wild-type distribution of INX-22 in the proximal gonad arm. (B) Dissected gonad arm of an F_1 animal from an *inx-14(RNAi)*-treated parent shows failure of INX-22 to localize to puncta in the proximal arm, as well as in the loop region (C) between distal (d) and proximal (p) arms. (D and E) The hypomorphic *inx-14(ag17)* mutation disrupts localization of INX-8/9, INX-21, and INX-22 to puncta (distal arm is shown); INX-8/9 is more diffusely distributed in the sheath, and coverage of germ cells by the sheath extends to the DTC. (F) In *inx-22(tm1661)* mutants, INX-8/9 and INX-14 colocalize to puncta in the distal gonad (d) but are diffusely distributed in the proximal gonad (–1, most proximal oocyte). (G) INX-21 distribution is unaffected in the distal arm of *inx-22 (tm1661)* mutants (pachytene region shown). (H and I) Injection of *inx-8* dsRNA into *inx-9(ok1502)* results in progeny with mislocalized germline innexins. Dissected gonads show loss of localization of INX-14 and INX-22 in the proximal region (H) and in the distal arm (pachytene region shown) (I). Bars, 20 μm. A summary of the interdependence of innexin colocalization is shown in Figure S5.

detected (Figure 8A), raising the question of how sheath components might end up in fertilized embryos. Vesicles that appear to consist of internalized gap junctions have been described in vertebrates and termed "annular junctions" (Larsen *et al.* 1979; Jordan *et al.* 2001), and internalization may involve a clathrin-mediated process (Piehl *et al.* 2007). We wondered if the presence of INX-8/9 in ovulating oocytes might represent annular junction formation.

Whole mounts or dissected gonads were stained with antibodies, and oocytes that appeared to have been ovulated into the spermatheca and presumably dissociated from the sheath were identified. Antibodies stained these oocytes prior to eggshell formation, and colocalization signals for both somatic and germline innexins were detected (Figure 8B). In *inx-22(tm1661)* mutants, the appearance of sheath innexins in ovulated oocytes is greatly reduced compared to wild type (Figure 8, C and D); presumably, the faint INX-8/9 signal detected in these embryos is due to INX-21 activity. Unlike colocalizing innexin signals in proximal oocytes, which are predominantly detected in focal planes consistent

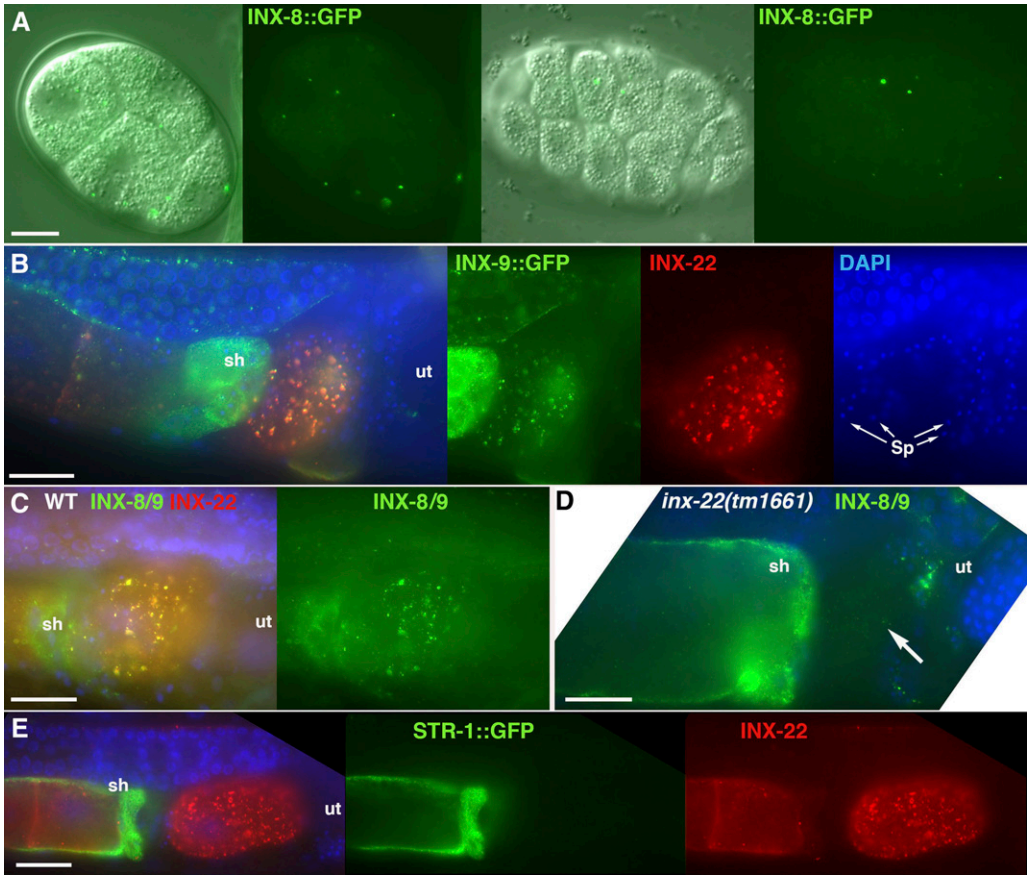

Figure 8 Sheath-expressed innexins are endocytosed by ovulating oocytes. (A) INX-8::GFP is detected in early embryos. (B) INX-22 and INX-9::GFP colocalize to internalized puncta in the oocyte after ovulation into the spermatheca (Sp, sperm nuclei). (C) INX-8/9 colocalizes with INX-22 in ovulated oocytes in the wild type, but is only weakly detected in *inx-22(tm1661)* ovulated oocytes (D). (E) *inx-8* promoter-driven expression of membrane-localized STR-1::GFP (*inx-8p::str-1::gfp)* fails to localize with INX-22 puncta internalized by the oocyte after ovulation. sh, sheath; ut, uterus. Bars, 20 μm.

with a cortical position, signals in ovulated oocytes were distributed throughout the cell.

INX-8/9 signals detected in ovulated oocytes could represent annular junctions formed as a means of resolving gap junctions shared between soma and the germ line at the time of ovulation, or they might represent a more general endocytosis of membrane components by the maturing oocyte. To distinguish between these possibilities, a nonjunctional membrane protein, STR-1::GFP, was expressed in the sheath using the *inx-8* promoter. STR-1 is a seven-transmembrane receptor protein (Troeml *et al.* 1997). STR-1::GFP expression was detected in the sheath, especially the proximal sheath, but was undetectable in ovulated oocytes (Figure 8E). Therefore, an association with germ cell innexins is required for sheath innexins to be endocytosed by ovulating oocytes.

inx-8 inx-9 and inx-22 inx-21 double mutants phenocopy inx-14 mutants

inx-14(tm2864) animals produce a small number of germ cells that become necrotic in adults. If INX-14 localization and function is dependent on INX-8/9 in the soma and INX-21 or INX-22 in the germ line, then the simultaneous loss of *inx-8* and *inx-9*, or of *inx-21* and *inx-22*, should at a minimum phenocopy *inx-14(tm2864)* sterility. To verify this, we sought to isolate the respective double mutants. Because both pairs of genes reside in tandem duplications, screens were initiated with a single mutation in one gene of each pair.

Briefly, to isolate *inx-8 inx-9* double mutants, a *sem-3(n1655) inx-9(ok1502)* strain was first constructed. *sem-3* mutant animals have defects in egg-laying muscles and retain most of the eggs they produce, resulting in fertile adults bloated with eggs that hatch inside the parent. The basis for the screen was the isolation of *sem-3 inx-9* animals that did not bloat with eggs, indicating the presence of a linked sterile or lethal mutation (see *Materials and Methods*). We screened for candidates that phenocopied *inx-14(tm2864)* as potentially representing *sem-3 inx-8 inx-9* mutants.

Two new mutations in *inx-8* linked to *inx-9(ok1502)* were isolated from ~4200 mutagenized chromosomes (Figure 9A). *inx-8(tn1474)* is a likely null allele that has a 312-bp deletion eliminating most of the predicted intracellular loop and much of the second extracellular loop (EL2) of INX-8 (ΔV135-V238). Hermaphrodites homozygous for *inx-8(tn1474) inx-9(ok1502)* are sterile and produce fewer germ cells than *inx-14(tm2864)* (Figure 9D). Males are also sterile. *inx-8(tn1513)* is a T239I missense mutation in EL2. The altered threonine lies close to one of the invariant cysteines found in EL2 of all innexins (C241 for INX-8). *inx-8(tn1513) inx-9(ok1502)* animals are sterile, but produce more germ cells per gonad arm than *inx-8(tn1474) inx-9(ok1502)* mutants. Mutant phenotypes of *inx-8(tn1474) inx-9(ok1502)* animals are rescued by extrachromosomal arrays carrying the *inx-8(+) inx-9(+)* genomic region, *inx-8::gfp*, or *inx-9::gfp*. We also rescued *inx-8(tn1513) inx-9(ok1502)* with

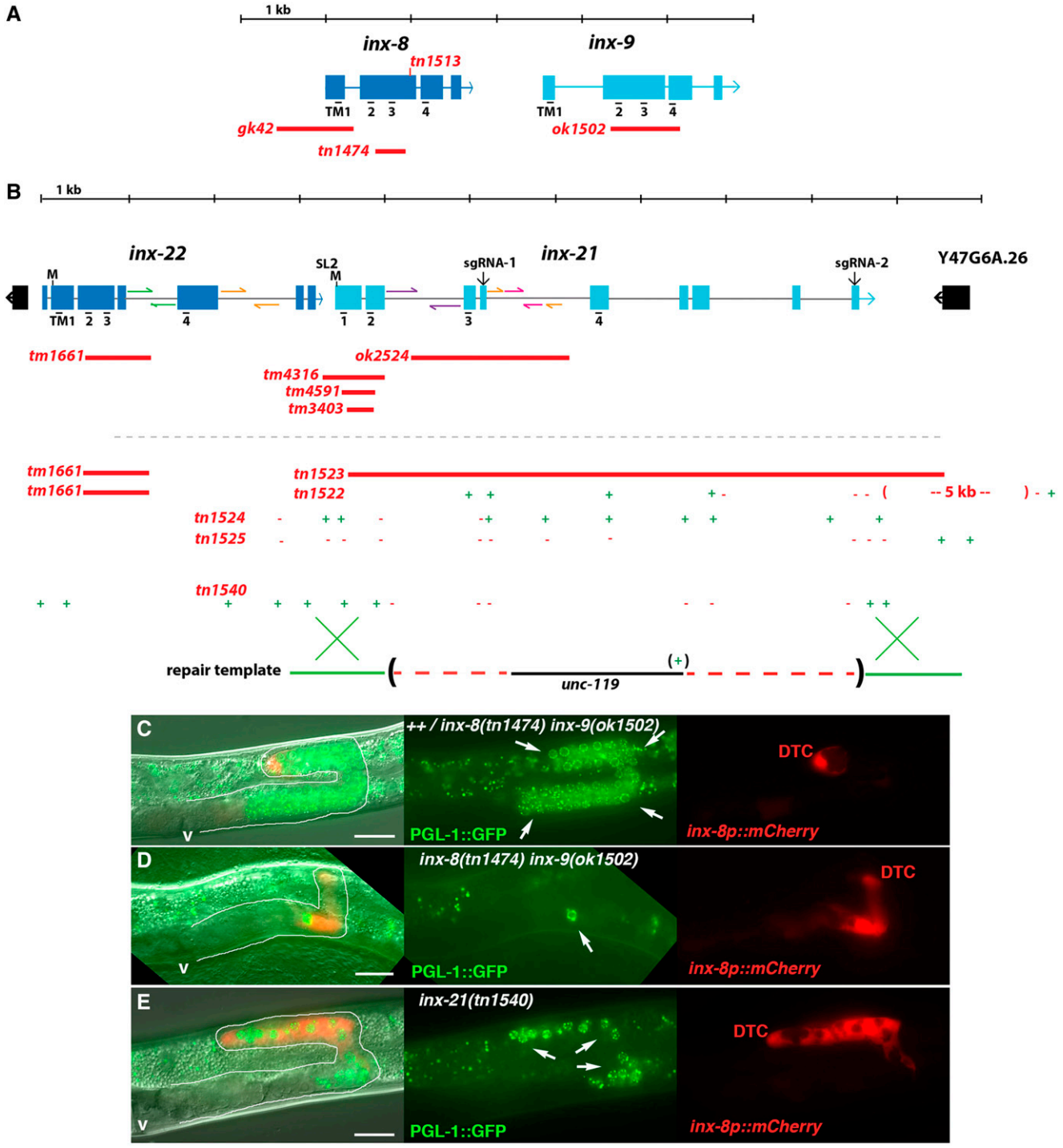

Figure 9 Mutational analysis of tandem gene duplications *inx-8/inx-9* and *inx-22/inx-21*. (A) *inx-8(gk42)* and *inx-9(ok1502)* mutants exhibit no apparent fertility phenotypes. A screen for *inx-14*-like sterility in an *inx-9(ok1502)* background generated the new *inx-8* alleles *tn1474* and *tn1513*. (B) *inx-22(tm1661)* and *inx-21* alleles *ok2524*, *tm3403*, *tm4316*, and *tm4591* do not markedly affect fertility. Two sgRNA sites in *inx-21* for directed CRISPR-Cas9 nuclease activity were used in either an *inx-22(tm1661)* background (to generate *tn1522* and *tn1523*) or a wild-type *inx-22* background (generating *tn1524*, *tn1525*, and *tn1540*). *tn1540* was generated using a repair template carrying the *unc-119(+)* gene in the *unc-119(ed3)* mutant background. Mutant alleles were evaluated by PCR analysis; sites of primer binding leading to a PCR product are indicated (+) and sites that appear to be deleted in the new alleles (–) are indicated. Because of the presence of numerous inverted repeats in introns at the locus (indicated as half-headed arrows; similar colors indicate sequence similarity), PCR assays in the region are problematic. Location of predicted TM domains in exon sequences are indicated. (C) Germline proliferation is unaffected in heterozygous *inx-8(tn1474) inx-9(ok1502)/++* animals, as assayed by the number of PGL-1::GFP-positive germ cells (arrows). Gonad arm of an L4 animal is outlined. (D) Homozygous *inx-8(tn1474) inx-9(ok1502)* mutants produce single-digit numbers of PGL-1::GFP-positive germ cells per animal (see Table 1). Gonad arm of an adult is outlined. (E) *inx-21(tn1540)* mutants produce an average of 18 ± 5 PGL-1::GFP-positive germ cells per gonad arm. Gonad arm of an adult is outlined. *inx-8p::mCherry* visualizes position of the DTC and sheath. Position of the vulva (v) is indicated. Bars, 20 μm.

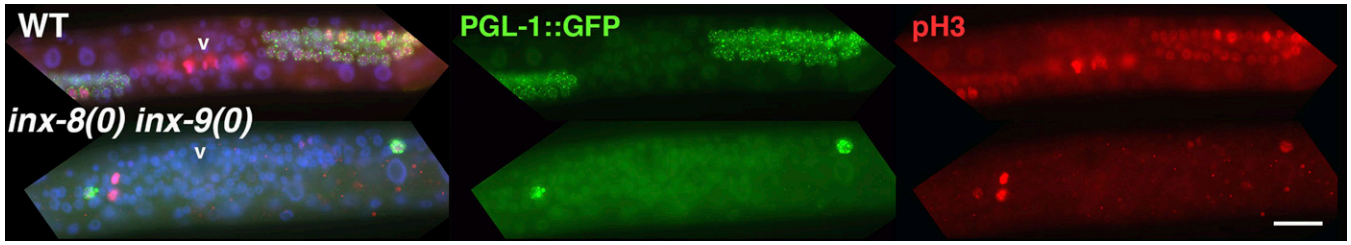

Figure 10 Germ cells fail to proliferate in *inx-8(tn1474) inx-9(ok1502)* mutants. Ventral views of wild-type (WT) and *sem-3(n1655) inx-8 inx-9* mutant worms at approximately equivalent larval stages (late L2/early L3). Germ cells marked with PGL-1::GFP (green) fill the developing wild-type gonad arms; both arms in this *inx-8 inx-9* mutant have a single PGL-1::GFP-positive germ cell. The M-phase marker anti-phospho-H3 staining (red) produces a weak signal with germ cells in *inx-8 inx-9* mutants. The position of developing vulva (v) is indicated. DAPI staining for cell nuclei is in blue. Bar, 20 μm.

inx-8::*gfp*. Further characterization of *inx-8 inx-9* mutants is described below.

To generate *inx-22 inx-21* double mutants, we used the recently developed CRISPR-Cas9 methodology for site-directed mutagenesis in *C. elegans* (Dickinson *et al.* 2013; Friedland *et al.* 2013; Tzur *et al.* 2013). Two sites in *inx-21* were targeted for cleavage with sgRNAs in *inx-22(tm1661)* animals, and potential new *inx-22 inx-21* double mutants produced by nonhomologous repair were isolated based on phenotypic similarity to *inx-14(tm2864)*. Two of 165 transgenic F_1 animals segregated sterile progeny that phenocopied *inx-14(tm2864)*. Both new *inx-21* mutations linked to *inx-22(tm1661)* are large deletions in the region: *inx-21(tn1522)* removes ~2 kb of *inx-21* sequence and at least 5 kb of adjoining sequence affecting two adjacent genes (Y47G6A.26 and Y47G6A.32), and *inx-21(tn1523)* is an ~7-kb deletion (with a novel 34-nt insertion) that removes most of *inx-21* and ~100 nt from the carboxyl terminus of Y47G6A.26 (Figure 9B). The phenotypes of *inx-22(tm1661) inx-21(tn1522)* and *inx-22 (tm1661) inx-21(tn1523)* homozygotes were comparable to *inx-14(tm2864)* animals, producing a small number of germ cells that failed to undergo gametogenesis and appeared necrotic in adults.

Mutation of inx-21 alone phenocopies inx-14

We evaluated whether the viable and fertile *inx-21* deletion alleles (*ok2524*, *tm3403*, *tm4316*, and *tm4591*) isolated by the Knockout Consortium represent null alleles. Each of these alleles deletes N-terminal INX-21 sequences, including at least one TM domain (Figure 9B). There are extensive inverted repeats found throughout the *C. elegans inx-22 inx-21* locus that make PCR assays in the region problematic and may account for the lack of fosmid or cosmid clones for the region. Examination of *inx-22* and *inx-21* sequences revealed that the fifth exons in both genes share the same reading frame and encode similar topological domains (predicted fourth TM domain and carboxyl terminus). Theoretically, all these deletion mutations limited to *inx-21* could produce a hybrid N-terminal INX-22/C-terminal INX-21 molecule that might react with C-terminal-targeted anti-INX-21 antibodies and rescue *inx-21* function. Indeed, antibodies raised against the carboxyl terminus of INX-21 were found to detect a product that colocalized with INX-22 in *inx-21(ok2524)* and *inx-21(tm4316)* mutants (Figure S4). This result is consistent with translation of an *inx-21* product in these deletion mutants. The production of a hybrid *inx-22–inx-21* mRNA in the wild type is not supported by an analysis of existing expressed-sequence tags, and initial attempts to identify a hybrid complementary DNA in the wild type by RT-PCR were unsuccessful (T. Starich, unpublished results). Thus, if a hybrid mRNA forms, it may be limited to the mutant backgrounds, which is a possibility we did not test.

The possibility that none of the extant *inx-21* mutants represented a true null allele was therefore explored. The same sgRNAs used to target *inx-21* in *inx-22* mutants were used in a wild-type background, and progeny were screened for producing an *inx-14(tm2864)*-like phenotype. Two new deletions affecting *inx-21*, *tn1524* and *tn1525*, were isolated, but again these deletions were not limited to the *inx-21* gene and *tn1524* might represent a rearrangement (Figure 9B). We therefore used CRISPR-Cas9-mediated homologous repair in an *unc-119(ed3)* mutant background to isolate a defined *inx-21* deletion, selecting for *unc-119* rescue. The repair template included *unc-119(+)* flanked on either side by 1 kb of *inx-21* sequence (Figure 9B). Homologous repair from this template is predicted to generate an *inx-21* deletion that removes the intracellular loop, EL2, and all but the most extreme C-terminal sequences of INX-21. We obtained a single *unc-119*-rescued animal, which segregated progeny displaying an *inx-14(tm2864)*-like phenotype. PCR analyses showed that these progeny lack *inx-21* sequences deleted from the repair template but maintain all other *inx-21* sequences flanking *unc-119* (Figure 9B), consistent with a deletion generated by homologous repair. PCR analysis of sequences in *inx-22* detected no anomalies (Figure 9B). Similar to *inx-14* and *inx-22 inx-21* double mutants, *inx-21(tn1540)* mutants produce a small number of germ cells by the L4 stage (18 ± 5 per gonad arm, range 9–31, $n = 19$) that become necrotic in adults (Figure 9E and Figure S6). Notably, the sterile phenotype of *inx-22 inx-21* double mutants is no more severe than *inx-21(tn1540)* single mutants. Taken together, the sterility of *inx-21(tn1540)* and the fertility of *inx-22(tm1661)* suggest that INX-21 is chiefly responsible for associating with INX-14 in germline hemichannels essential for germline proliferation. Therefore, the functions of the different soma–germline gap junction channels appear to be determined by the alternative inclusion of INX-21 or INX-22.

Table 1 ***inx-8(tn1474) inx-9(ok1502)*** **mutants exhibit a severe germline proliferation defect**

	Average no. of germ cells per animal[a]			
Genotype	L2–L3	L3–L4	L4–YA	Adult
WT	76 ± 21 (n = 12)	186 ± 37 (n = 9)	~1000[b]	~2000[b]
inx-8 inx-9	5.3 ± 3.3 (n = 39)	7.4 ± 5.9 (n = 11)	3.3 ± 1.6 (n = 24)	2.5 ± 2.3 (n = 13)

[a] The number of germ cells was determined by anti-GFP staining of PGL-1::GFP-positive germ cells in *sem-3(n1655) inx-8(tn1474) inx-9(ok1502); nels5[pgl-1::gfp]* animal whole mounts from mixed-stage cultures. Larval, young adult (YA), and adult stages were approximated by DAPI staining.
[b] Germ cell numbers are from Francis *et al.* (1995b) and are presented for comparison.

inx-8 inx-9 mutants have defects in germ cell proliferation

Because *inx-8* and *inx-9* appear to be required for the localization of INX-14, INX-21, and INX-22 to presumptive gap junctions (*i.e.*, puncta; see Figure 7 and Figure S5), we focused on characterizing *inx-8(tn1474) inx-9(ok1502)* mutants as representative of the phenotypes resulting from loss of all INX-8/9-based gap junction coupling between soma and the germ line. The presence of only a few germ cells in *inx-8 inx-9* animals could result from a defect in proliferation or a problem with cell maintenance after division. To assess this, we used DIC microscopy to examine Z2 and Z3 in living *inx-8(tn1474) inx-9(ok1502)* animals from the mid-L1 larval stage to early L2. During this time in wild-type animals, germ cells have typically undergone multiple divisions, and descendants of somatic gonad precursors Z1 and Z4 have divided to generate 12 somatic cells (Kimble and Hirsh 1979). Cell divisions in five gonads of *inx-8(tn1474) inx-9(ok1502)* mutants were followed; in total, two Z2 and no Z3 division events were observed by the early L2 stage. By contrast, Z1 and Z4 divisions occurred apparently normally. Because *inx-8(gk42)* and *inx-9(ok1502)* single mutants are fertile, these results demonstrate that *inx-8* and *inx-9* are redundantly required for early germ cell proliferation.

To extend this, we used the PGL-1::GFP marker, which is expressed in all germ cells (Kawasaki *et al.* 1998), to estimate germ cell numbers in *inx-8(tn1474) inx-9(ok1502)* animals at different developmental stages (Figure 10 and Table 1). Average germ cell numbers peaked during mid-to-later larval stages (~7.4 per animal, range 2–19; Table 1). In 16% of larvae (12/74), germ cells could be detected only in one gonad arm of an animal. In adults, the numbers of PGL-1::GFP-positive cell numbers decreased, and PGL-1::GFP expression appeared diffuse, possibly reflecting the necrosis of germ cells that is observed at this stage (Figure S6). To assess germ cell division further, we used phospho-histone H3 antibodies as a marker for mitotic divisions and examined *inx-8(tn1474) inx-9(ok1502)* mutants bearing the PGL-1::GFP marker. Most *inx-8(tn1474) inx-9(ok1502)* germ cells were weakly positive for expression of phospho-H3 and did not exhibit the staining intensity seen in dividing wild-type germ cells (Figure 10). Possibly, germ cells in *inx-8(tn1474) inx-9(ok1502)* mutants arrest at a common stage. Because germline proliferation depends upon INX-8 and INX-9, which are expressed in the somatic gonad, and INX-14 and INX-21, which are expressed in the germ line, we conclude that INX-8/INX-9: INX-14/INX-21 gap junctions are required for germline proliferation.

The average number of germ cells produced in *inx-8 (tn1474) inx-9(ok1502)* mutants is similar to that reported for strong loss-of-function *glp-1/Notch* mutants (Austin and Kimble 1987). GLP-1/Notch signaling in germ cells promotes proliferation (Austin and Kimble 1987, 1989; Yochem and Greenwald 1989) when activated by its ligands LAG-2/Delta and APX-1, produced by the DTC (Henderson *et al.* 1994; Tax *et al.* 1994; Nadarajan *et al.* 2009). In the absence of *glp-1/Notch* signaling, the few germ cells produced are able to differentiate, and they enter meiosis one stage early (L2/L3 molt) to produce fully functional sperm (Austin and Kimble 1987). By contrast, we have not observed evidence of differentiation (meiotic entry or gametogenesis) in *inx-8(tn1474) inx-9(ok1502)*, *inx-14(tm2864)*, or *inx-21(tn1540)* mutants. To test the possibility that *inx-8(tn1474) inx-9(ok1502)* germ cells are competent to differentiate but are prevented from doing so due to active *glp-1/Notch* signaling, we examined *inx-8(tn1474) inx-9(ok1502)*; *glp-1(q46)* triple mutants. A dominantly marked *inx-8 inx-9* chromosome was used to isolate *glp-1(q46)*; *inx-8(tn1474) inx-9(ok1502) mIs11(gfp+)* animals. No evidence of germ cell differentiation to sperm was seen in 20 animals examined, in contrast to *glp-1(q46)*; *inx-8(tn1474) inx-9(ok1502)/++* controls in which sperm were evident (Figure 11A). Therefore, it appears that *inx-8 inx-9* germ cells are not competent for differentiation.

Loss of gap junctions between germ cells and soma is epistatic to germ cell proliferation-promoting mutations

Soma–germline gap junctions are required for normal germ cell proliferation. Thus we examined the epistatic relationships between this function and other mediators of germ cell proliferation. GLP-1/Notch signaling in germ cells promotes proliferation. The gain-of-function *glp-1(oz112)* mutant allele encodes a constitutively active ligand-independent form of GLP-1/Notch that causes a tumorous germ cell phenotype (Berry *et al.* 1997; Hansen *et al.* 2004a). Again we used the dominantly marked *inx-8 inx-9* chromosome to isolate *glp-1 (oz112)*; *inx-8(tn1474) inx-9(ok1502) mIs11(gfp+)* animals. All of these animals displayed the *inx-8(tn1474) inx-9(ok1502)* sterile phenotype (n = 16), and there was no evidence of germline tumor formation (Figure 11B). In contrast, all *glp-1(oz112)*; *inx-8(tn1474) inx-9(ok1502)/++* heterozygous animals (n = 32) produced germ cell tumors (Figure 11B).

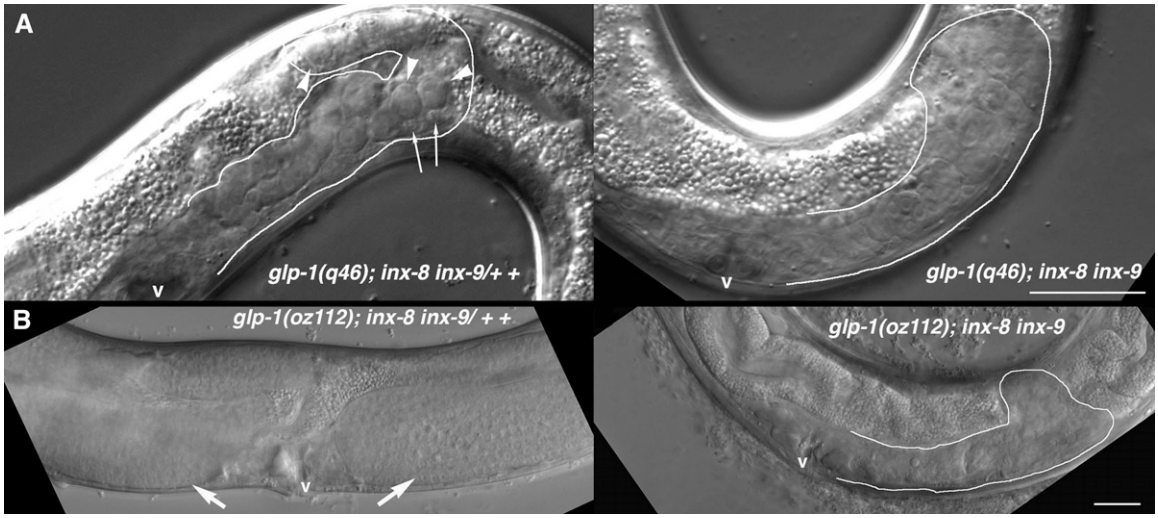

Figure 11 *inx-8 inx-9* is epistatic to recessive and dominant *glp-1* mutations. (A) *unc-32(e189) glp-1(q46)*; *sem-3(n1655) inx-8(tn1474) inx-9(ok1502) mIs11(gfp+)/++++* gonads produce few germ cells, but those germ cells can differentiate to sperm. Arrows indicate sperm, and arrowheads indicate residual bodies, produced during spermatogenesis (Ward *et al.* 1981). Germ cells in *unc-32(e189) glp-1(q46)*; *sem-3(n1655) inx-8(tn1474) inx-9(ok1502) mIs11(gfp+)* homozygotes do not generate sperm. (B) *unc-32(e189) glp-1(oz112)*; *sem-3(n1655) inx-8(tn1474) inx-9(ok1502) mIs11(gfp+)/++++* animals produce germline tumors, but germ cells do not proliferate in *unc-32(e189) glp-1(oz112)*; *sem-3(n1655) inx-8(tn1474) inx-9(ok1502) mIs11(gfp+)* homozygotes. Gonad arms are outlined and the position of the vulva (v) is indicated. Bars, 20 μm.

Therefore, *inx-8(tn1474) inx-9(ok1502)* is epistatic to *glp-1(oz112)*, and somatic INX-8/9 is required for activated GLP-1 to exert its effects.

GLP-1/Notch signaling is dispensable for germline proliferation upon inactivation of the genes *gld-1* and *gld-2*, which regulate entry into the meiotic pathway of development. In *gld-2 gld-1*; *glp-1* mutants, synthetic germ cell tumor formation occurs in a *glp-1*-independent manner (Kadyk and Kimble 1998; Hansen *et al.* 2004b). *gld-1* encodes an RNA-binding protein that negatively regulates translation of many of its mRNA targets (Jones and Schedl 1995; Jan *et al.* 1999; Lee and Schedl 2001; Jungkamp *et al.* 2011; Wright *et al.* 2011; Doh *et al.* 2013); *gld-2* encodes the catalytic subunit of a cytoplasmic poly(A) polymerase that may stabilize and promote the expression of its mRNA targets (Wang *et al.* 2002; Kim *et al.* 2010). To determine if soma–germline gap junctions might be required for *gld-2 gld-1* tumor formation, RNAi knockdown of *inx-14* was carried out by microinjection of *inx-14* dsRNA into a *gld-2(q497) gld-1(q485)/++*; *glp-1 (q175)/+* genetic background. All *gld-2 gld-1*; *glp-1* progeny of uninjected adults gave rise to germline tumors (n = 30). By contrast, 15/20 *gld-2 gld-1*; *glp-1* progeny from *inx-14(RNAi)*-treated adults failed to produce germline tumors and displayed an *inx-14(tm2864)*-like phenotype. Therefore soma–germline gap junctions are still required in a genetic background in which GLP-1/Notch signaling is dispensable for germ cell proliferation.

Expression of INX-8 in the DTC rescues germ cell proliferation and gametogenesis in inx-8 inx-9 mutants

Characterization of innexin mutants showed that there are at least two functions mediated by soma–germline gap junctions: an early distal arm function is required for germ cell proliferation and differentiation and a later proximal arm function in the negative regulation of oocyte meiotic maturation in the absence of sperm. Studies of meiotic maturation inhibition were based on use of *inx-22* mutants or *inx-14(RNAi)* (Govindan *et al.* 2006, 2009; Whitten and Miller 2007). In these backgrounds, not all soma–germline gap junctions were absent, since complete elimination of INX-14 results in few germ cells, and we now show that INX-21 also contributes to such junctions. Therefore, we sought to rescue distal proliferation in a way that allowed investigation of the consequences of losing all proximal INX-8/9-based soma–germline gap junctions.

Expression of *lag-2* in the adult gonad is restricted to the DTC (Henderson *et al.* 1994; Fitzgerald and Greenwald 1995). A *lag-2p*::*inx-8*::*gfp* transgene efficiently rescues germ cell proliferation and gametogenesis in essentially all *inx-8(tn1474) inx-9(ok1502)* animals. Proliferation is rescued to a large degree such that adult gonad arms contained 523 ± 5 germ cells (n = 3) compared to >1000 in the wild type (McCarter *et al.* 1997). Expression of *lag-2p*::*inx-8*::*gfp* was detected in the DTC cell body as well as long processes that extended over many germ cell diameters (Figure 12, A and B). In this genetic background, germ cell innexins colocalized with INX-8::GFP expressed in the DTC (Figure 12, B and D), but failed to localize to organized puncta in the pachytene region or proximal arm (Figure 12, C and D), consistent with loss of INX-8/9 in these regions.

With no apparent proximal soma–germline gap junctions forming, *inx-8(tn1474) inx-9(ok1502)*; *tnEx205[lag-2p*::*inx-8*::*gfp]* animals were examined for oocyte phenotypes. We predicted that these animals would, like *inx-22(tm1661)* mutants, fail to properly inhibit meiotic maturation in a female background (*i.e.*, in the absence of the MSP meiotic maturation signal

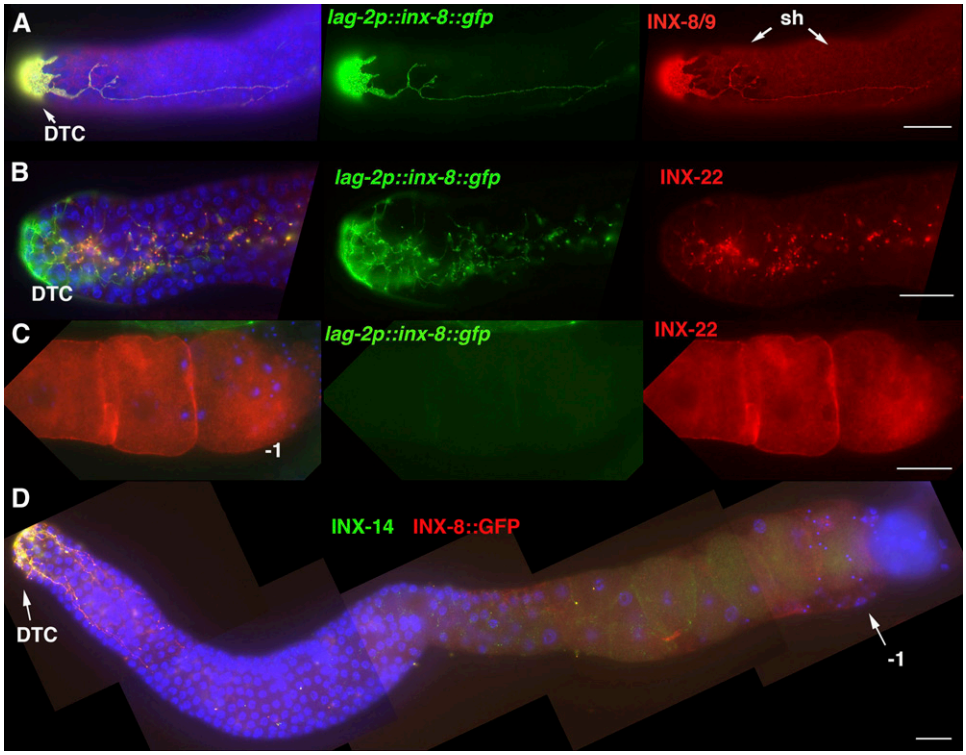

Figure 12 Expression of *lag-2p*::*inx-8*::*gfp* rescues germ cell innexin localization in the distal arm but not in the proximal arm in *inx-8(tn1474) inx-9(ok1502)* mutants. (A) Upper focal plane of a dissected gonad co-stained with anti-GFP to detect INX-8::GFP expression in the DTC (green) and with anti-INX-8 (red), which also detects INX-8::GFP. Background staining from the secondary antibody used to detect anti-INX-8 enabled visualization of the sheath (sh). Note that the sheath coverage of germ cells extends distally as far as the DTC, as was also observed in *inx-14(ag17)* animals (see Figure 7D), possibly as a consequence of submaximal proliferation. (B and C) The germline innexin INX-22 colocalizes with DTC-expressed INX-8::GFP, visualized in a medial focal plane in B, but does not localize to puncta in the proximal gonad arm (C). (D) The germline innexin INX-14 (green) also colocalizes with DTC-expressed INX-8::GFP (red, detected using anti-INX-8) only in the region of the DTC. The most proximal oocyte (–1) is indicated. Bars, 20 μm.

from sperm) (Govindan *et al.* 2006, 2009; Whitten and Miller 2007). *fog-2(oz40)* XX animals are feminized and produce no sperm (Schedl and Kimble 1988). In unmated *fog-2(oz40)* female animals, oocytes stack in the proximal arm, and diphosphorylated activated mitogen-activated protein kinase (MAPK), a readout of MSP signaling, is also largely absent from oocytes (Figure 13A). In unmated *fog-2(oz40)*; *inx-8(tn1474) inx-9(ok1502)*; *tnEx205[lag-2p*::*inx-8*::*gfp]* animals, oocytes do not stack but instead undergo meiotic maturation and ovulation (Figure 13, C and D). These ovulated but unfertilized oocytes become endomitotic in the uterus as expected (Figure 13, C and D; Ward and Carrel 1979). Dissected gonad arms from these animals show evidence of MAPK activation in proximal oocytes (Figure 13B). These results support the conclusion that expression of INX-8::GFP in the DTC of *inx-8(tn1474) inx-9(ok1502)* mutants is sufficient to establish functional gap junctions distally but not proximally. The distal soma–germline gap junctions appear sufficient to promote substantial germline proliferation and gametogenesis. In the absence of soma–germline gap junctions, oocyte meiotic maturation occurs constitutively in the absence of sperm, as was observed in *inx-22(tm1661)* or *inx-14(RNAi)* females (Govindan *et al.* 2006, 2009; Whitten and Miller 2007). We conclude that INX-8/INX-9:INX-14/INX-22 junctions between sheath cells and oocytes mediate the inhibition of meiotic maturation in the absence of sperm.

We also examined if *inx-8(tn1474) inx-9(ok1502)*; *tnEx205[lag-2p*::*inx-8*::*gfp]* males were rescued for germ cell proliferation. Individual males were plated with *unc-29*; *mIs11* hermaphrodites; 6 of 10 males produced cross-progeny (average 61 ± 61, range 9–156), indicating that DTC expression of INX-8::GFP is capable of restoring appreciable germline proliferation, gametogenesis, and fertility to *inx-8 inx-9* males.

Proximal arm gap junctions are required for embryonic viability

In contrast to *inx-22* mutants, *inx-8(tn1474) inx-9(ok1502)*; *tnEx205[lag-2p:inx-8:gfp]* animals have additional proximal arm defects. These animals produce small numbers of fertilized embryos, almost none of which hatch to give viable larvae (avg. 0.4 ± 0.9, n = 36). Many embryos display phenotypes associated with *pod* (**p**olarity and **o**smotic sensitivity **d**efects) mutants exhibiting eggshell defects, such as *gna-2* (Johnston *et al.* 2006), *cpg-1*, *cpg-2* (Olson *et al.* 2006), *chs-1* (Zhang *et al.* 2005), and *syx-4* (Jantsch-Plunger and Glotzer 1999). These defects can lead to failures in cytokinesis, polar body extrusion, and dye exclusion.

The eggshells of most wild-type embryos exclude DAPI (Figure 14A). In early embryos dissected from wild-type hermaphrodites, only a single one-cell embryo, presumably isolated before eggshell synthesis was complete, failed to exclude DAPI (n = 28). In embryos dissected from *inx-8(tn1474) inx-9(ok1502)*; *tnEx205[lag-2p:inx-8:gfp]* animals, 50% (n = 30) failed to exclude DAPI (Figure 14B), 41% (n = 37) exhibited cytokinesis defects (Figure 14C), and polar body extrusion defects were noted but not quantified (Figure 14D).

gna-2 mutants lack glucosamine-6-phosphate *N*-acetyltransferase, an enzyme critical in the pathway leading to eggshell chitin synthesis, but can be partially rescued by injection of UDP-GlcNac into the gonad arm (Johnston *et al.* 2006). We hypothesized that sheath–oocyte gap junctions

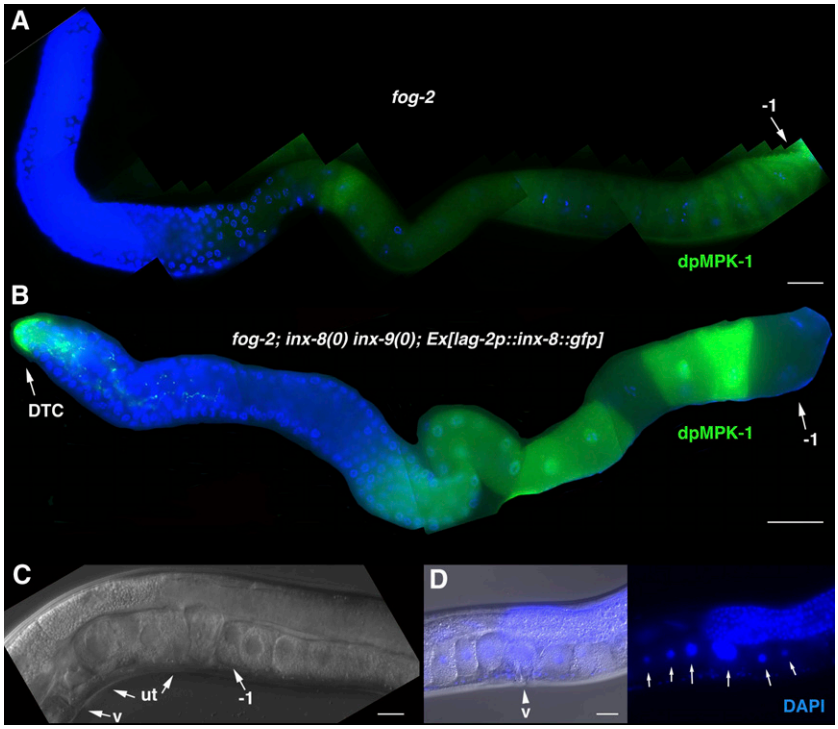

Figure 13 *inx-8 inx-9* mutant proximal gonadal sheath cells are defective for inhibition of meiotic maturation in the absence of sperm. (A) Oocytes in *fog-2(oz40)* unmated females stack and exhibit little evidence of MAPK activation as detected by an antibody specific for the diphosphorylated form of the enzyme (dpMPK-1). (B–D) Oocytes in unmated *fog-2(oz40); sem-3(n1655) inx-8(tn1474) inx-9(ok1502); tnEx205[lag-2p::inx-8::gfp]* females exhibit MAPK activation (B), are ovulated into the uterus (C), and become endomitotic (D). The most proximal oocyte (–1) and the positions of the DTC, vulva (v), and uterus (ut) are indicated. DAPI staining of nuclei is in blue. Bars, 20 μm.

might be critical for supplying components to the oocyte essential for eggshell formation. UDP-GlcNac is a necessary component late in the pathway leading to chitin synthesis; therefore, if the sheath is required to provide any earlier components of the chitin synthesis pathway to the oocyte, this requirement might be complemented by addition of UDP-GlcNac. We injected UDP-GlcNac into *inx-8(tn1474) inx-9(ok1502)*; *tnEx205[lag-2p::inx-8::gfp]* gonad arms, but no sign of rescue of embryonic viability was seen (Table S1). As a control, we replicated the rescue of *gna-2(qa705)* mutants by UDP-GlcNac injection (Table S1).

To test whether *inx-8(1474) inx-9(1502)*; *tnEx205 [lag-2p::inx-8::gfp]* embryonic defects might be rescued by proximal soma–germline gap junctions, an enhancer of *lim-7* (Voutev *et al.* 2009) was used to drive expression of *inx-8::gfp* in sheath cells in *inx-8(tn1474) inx-9(ok1502)* double mutants. Expression of the *lim-7p::inx-8::gfp* construct was first detected in the gonad at the approximate mid-late L3 larval stage, coincident with early signs of vulval invagination during morphogenesis. When *lim-7p::inx-8::gfp* was used in conjunction with *lag-2p::inx-8::gfp*, *inx-8(tn1474) inx-9(ok1502)* animals were rescued to fertility in established lines (average brood size 133 ± 43, range 42–241, $n = 30$; Figure 15A), and evidence for gap junction formation between sheath and oocyte was evident in the large amounts of sheath-expressed INX-8::GFP that could be detected in embryos (Figure 15B). This result confirms that an INX-8/9 sheath function is required for embryonic viability.

Most *inx-8(tn1474) inx-9(ok1502)* mutants that carried only *lim-7p::inx-8::gfp* were sterile (93%, $n = 215$). Of the gonad arms examined by DIC microscopy ($n = 65$), ~85% produced few germ cells, similar to *inx-8(tn1474) inx-9(ok1502)* mutants (Figure 15C); the remainder showed evidence of germ cell proliferation rescue to varying extents (Figure 15, D and E). Proliferation rescue ranged from a small bolus of germ cells to rescue of fertility, although a brood size >30 was produced by only 1% of these animals. We questioned whether *lim-7p::inx-8::gfp* might be stochastically expressed in earlier larval stages, but no evidence of *lim-7p::inx-8::gfp* expression was detected in L2 larvae ($n = 45$). We cannot exclude the possibility that earlier *lim-7p::inx-8::gfp* expression lies below our detection level; however, we noted that gonad arms in L2 animals showed little evidence of germ cell proliferation (average 1.6 germ cells per arm, range 0–3, $n = 8$), suggesting that the *lim-7p::inx-8::gfp* array provides minimal rescue of proliferation at a stage earlier than its expression is detected. Our interpretation of the stochastic nature of this rescue is that it represents the intersection of the time window of *inx-8 inx-9* germ cell persistence (Table 1) and competence to respond to proliferation cues with the earliest time of *lim-7p::inx-8::gfp* expression. This result further suggests that INX-8/9 sheath function may overlap its DTC function regarding germ cell proliferation.

DTC expression of INX-8 is sufficient but not necessary to rescue proliferation

DTC expression of *lag-2p::inx-8::gfp* appeared largely sufficient to rescue germ cell proliferation defects in *inx-8(tn1474) inx-9(ok1502)* mutants. Corroboration was provided by random examination of *inx-8(tn1474) inx-9(ok1502)*; *tnEx205[lag-2p::inx-8::gfp]* animals for expression of the *inx-8::gfp* array in the DTC and for the corresponding state of germ cell proliferation in each gonad arm. Of 532 gonad arms examined, 529 showed a coincidence of germ cell

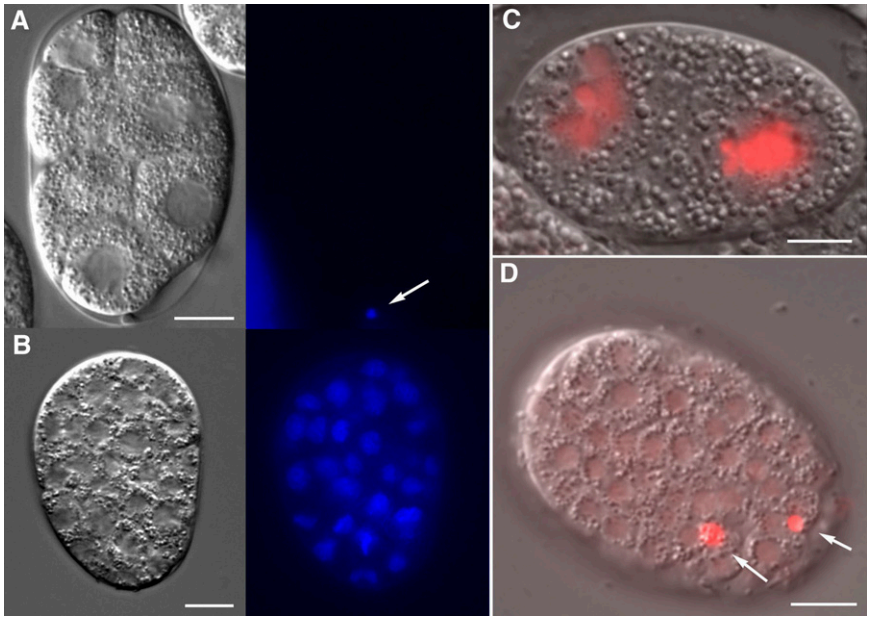

Figure 14 *inx-8(tn1474) inx-9(ok1502)*; *tnEx205 [lag-2p*::*inx-8*::*gfp]* embryos exhibit *pod* mutant phenotypes. (A) Eggshells in wild-type embryos exclude DAPI stain; only the first polar body, which is outside the permeability barrier (Olson *et al.* 2012), takes up the dye. (B) DAPI diffuses through the eggshells of many *inx-8(tn1474) inx-9(ok1502)*; *tnEx205[lag-2p*::*inx-8*::*gfp]* embryos and stains nuclei. (C) Failure in cytokinesis and (D) polar body extrusion in *inx-8(tn1474) inx-9(ok1502)*; *tnEx205 [lag-2p*::*inx-8*::*gfp]* embryos expressing mCherry::HIS-2B (*pie-1p*::*mCherry*::*his-48*) (Toya *et al.* 2010). Bars, 10 μm.

proliferation with *inx-8*::*gfp* expression in the DTC. The only exceptions included one animal with DTC expression in both arms that displayed a germ cell proliferation defect and one arm lacking *inx-8*::*gfp* expression in the DTC but still showing germ cell proliferation in that arm (the other gonad arm in that animal showed DTC expression from the array).

However, analysis of expression of the *inx-8* promoter region suggested that other somatic cells in addition to the DTC might express INX-8 at a developmental time that could promote germ cell proliferation (Figure 5, K and L). Genetic mosaic analysis was therefore used to determine if DTC expression of INX-8 is necessary for germ cell proliferation. *inx-8(tn1474) inx-9(ok1502)* mutants were rescued with an array carrying the *inx-8 inx-9* genomic region along with *sur-5*::*gfp*, which is expressed in all somatic cells and is commonly used as a tool for genetic mosaic analysis (Yochem *et al.* 1998; Yochem and Herman 2003). We screened ~5000 animals for genetic mosaicism of *inx-8 inx-9* within the somatic gonad (Figure 16). In each gonad arm, three spermathecal cells (as well as two spermathecal–uterine junction cells) are derived from progenitors that give rise to the other gonad arm (Kimble and Hirsh 1979). If one gonad arm showed the absence of *sur-5*::*gfp* expression in the DTC, all sheath cells, and all but three spermathecal cells, it was interpreted as a Z1 or Z4 loss. In most of the gonad arms examined, loss of the rescuing array was complex, but the presence or absence of the array in the DTC *vs.* other somatic gonad cells was scored (Figure 16).

Thirteen mosaic animals were identified that were informative. Eight gonad arms (class I) showed proliferation of germ cells and gametogenesis in a gonad arm that failed to express *sur-5*::*gfp* in the DTC but expressed the marker in other cells of that gonad arm. Another five gonad arms (class II) with germ cell proliferation represented probable complete Z1 or Z4 losses, but the opposite gonad arm in these animals expressed the array (although in two cases not in the DTC). By contrast, three presumptive Z1 losses led to sterile arms in animals that carried the array (and showed proliferation rescue) in the posterior arms (class III). Finally, one animal carried the array in descendants of both Z1 and Z4 but showed no signs of germ cell proliferation (class IV).

Together these results suggest that DTC expression of *inx-8 inx-9* is not an absolute requirement for germ cell proliferation, and other somatic gonad cells appear to express *inx-8 inx-9* (at least when provided in a multi-copy array) to levels that provide this function. Absolute germ cell numbers in gonad arms interpreted as proliferating were not determined, and there may be a difference in efficacy of proliferation rescue, depending on which cells carried the array. Interestingly, in several cases the proliferation of germ cells in one gonad arm lacking the array appeared to be rescued by INX-8::GFP expression in progenitors giving rise to the other gonad arm.

INX-8(T239I) localizes to presumptive gap junctions

The point mutation *inx-8(tn1513)* was isolated in the screen for *inx-8 inx-9* double mutants. We considered the possibility that this missense mutation affects channel function but not localization. *inx-8(tn1513) inx-9(ok1502)* mutants are sterile but produce more germ cells than *inx-8(tn1474) inx-9(ok1502)* animals, suggesting that *tn1513* is hypomorphic (Figure 17A). In *inx-8(tn1513) inx-9(ok1502)* animals, germ cell numbers can approach 100 in a single gonad arm (average 23 ± 20, median 18, range 2–115, $n = 76$), and in these infrequent cases sperm may differentiate as assessed by DAPI staining ($n = 4$). In adults, germ cells rarely form the necrotic foci seen in *inx-8(tn1474) inx-9(ok1502)* mutants, but

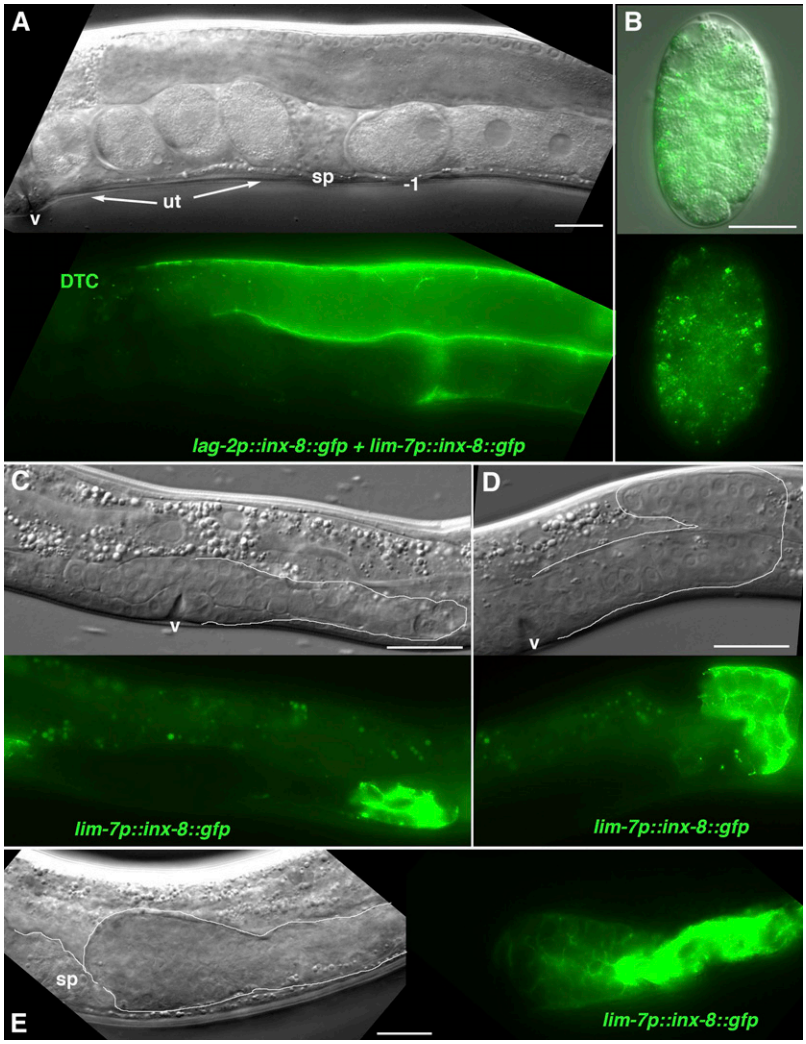

Figure 15 Sheath-expressed INX-8::GFP rescues *inx-8 inx-9*; *tnEx205[lag-2p::inx-8::gfp]* embryonic lethality. (A) *lim-7p::inx-8::gfp* is expressed in cells of the sheath lineage beginning at approximately the mid-L3 stage and, together with *lag-2p::inx-8::gfp*, can rescue *inx-8(tn1474) inx-9(ok1502)* animals to fertility. High expression levels of INX-8::GFP in the proximal sheath mask underlying INX-22 puncta formation as detected by immunostaining (T. Starich, unpublished results). (B) Embryos from rescued animals endocytose INX-8::GFP from the sheath. (C–E) In *inx-8(tn1474) inx-9(ok1502)* mutants, *tnEx202[lim-7p::inx-8::gfp]* alone inefficiently rescues germline proliferation to varying extents. (C) Lack of proliferation rescue produces an *inx-8(tn1474) inx-9(ok1502)*-like gonad arm. One gonad arm of an L4 animal is outlined. (D) Moderate germline proliferation allows for extension of a short gonad arm to the dorsal side (gonad arm of L4 is outlined). (E) A bolus of germ cells in the proximal region of an adult gonad arm (outlined). The spermatheca (sp), uterus (ut), and vulva (v) are indicated. Bars, 20 μm.

germ cell nuclei become difficult to distinguish by Nomarski optics (Figure 17B). Anti-INX-8 antibodies detected expression of INX-8(T239I) in *sem-3 inx-8(tn1513) inx-9(ok1502)* animals in a few gonads large enough to protrude out of dissected animals; in these cases it appeared that INX-22 colocalized with INX-8(T239I) to some extent (Figure 17C); however, it was difficult to distinguish if presumptive gap junction puncta might be formed.

To examine if INX-8(T239I) might localize to presumptive gap junctions, we utilized the *lag-2p::inx-8::gfp* construct to rescue germ cell proliferation in *sem-3 inx-8(tn1513) inx-9(ok1502)* animals. In this genetic background, INX-8(T239I) localized to small puncta in the distal sheath that tended to lie at germ cell borders and to rather large puncta in the proximal sheath (Figure 17D). Although somewhat difficult to distinguish against a strong diffuse distribution of INX-8(T239I) in the proximal sheath, these puncta are readily visualized by colocalization with INX-22 (Figure 17E). Because *lag-2p::inx-8::gfp* is not detected in the proximal arm, localization of INX-22 is facilitated by INX-8(T239I) (compare to Figure 12C). *sem-3 inx-8(tn1513) inx-9(ok1502)*; *tnEx205 [lag-2p::inx-8::gfp]* animals are not rescued for fertility, and therefore INX-8(T239I) function is compromised both for germ cell proliferation and proximal sheath functions.

Discussion

Five innexins establish soma–germline gap junctions

These results uncover new roles for gap junctions in supporting germline proliferation, gametogenesis, and early embryogenesis. Our model (Figure 18) is that INX-14 is present in all germ cell hemichannels, but it requires either INX-21 or INX-22 to form channels with somatic INX-8/9. Specificity of function appears to derive from the INX-14-associated partner, as likely null alleles of *inx-21* and *inx-22* exhibit different phenotypes. INX-21 is the principal partner of INX-14 in hemichannels required for germline proliferation. In addition, in *inx-8(tn1474) inx-9(ok1502)* mutants rescued for germline proliferation by expression of *inx-8::gfp* in the DTC, we also found that fertilized oocytes uncoupled to the sheath often display embryonic lethal phenotypes associated with eggshell synthesis mutants. Because *inx-22(tm1661)* mutants are viable and fertile, we favor the hypothesis that germline INX-14/INX-21 hemichannels associate with INX-8/9 in sheath

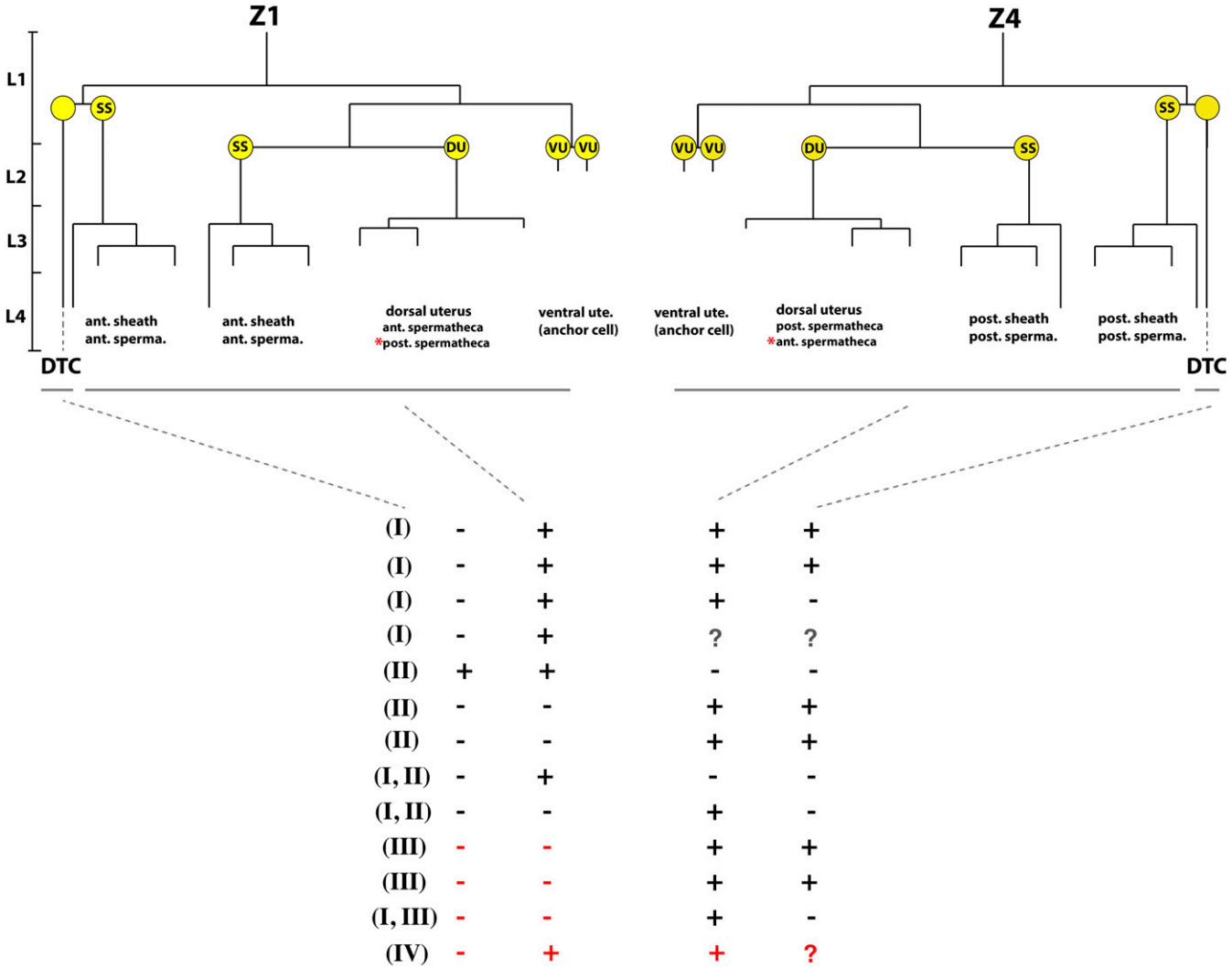

Figure 16 Genetic mosaic analysis suggests that somatic gonad cells other than the DTC can rescue germ cell proliferation in *inx-8 inx-9* mutants. Abbreviated cell lineage of each gonad arm (adapted from Kimble and Hirsh 1979) shows the somatic cells emerging by early L2 stage (yellow) and the structures to which their descendants contribute. In the anterior gonad arm, derived from Z1, three spermathecal cells (red asterisk) and two spermathecal-uterine junction cells (not shown) are derived from descendants of Z4, and a reciprocal contribution holds for the posterior arm. Cells of the somatic gonad were examined in individual *inx-8(tn1474) inx-9(ok1502); tnEx195[inx-8(+) inx-9(+); sur-5::gfp]* animals for the presence of the rescuing array carrying the cell-autonomous *sur-5::gfp* marker. Where possible, the DTC, sheath, and spermathecal cells were scored; if the DTC, all sheath cells, and all but three spermathecal cells were GFP(–), that gonad arm was scored as a probable Z1 or Z4 loss. The presence or absence of *sur-5::gfp* is indicated as "+" or "−." The presence of at least ~50 germ cells and gametes was taken as evidence of germ cell proliferation in a gonad arm, indicated in black type. All genetically mosaic gonad arms rescued for proliferation also produced gametes. Absence of proliferation (the *inx-8 inx-9* mutant phenotype) is indicated by red type. Gonad arms that could not be scored are indicated by a question mark (?). Classes of mosaic gonad arms (I–IV) are described in the text.

cells to form channels that function in the gonad, but are required for early embryonic events. Although the bulk of INX-14 expression does not localize to puncta in *inx-22(tm1661)* mutants, INX-8/9:INX-14/INX-21 channels still form and are functional. By contrast, INX-22 is required for the negative regulation of oocyte meiotic maturation and functions together with INX-8 and INX-9 in the sheath. INX-22 was previously shown to be required for the oocyte growth-promoting cytoplasmic flows to cease in the absence of the MSP signal (Govindan *et al.* 2009). *glp-1/Notch* and *inx-22* exhibit genetic interactions affecting oocyte growth; *inx-22* enables elevated rates of cytoplasmic streaming in the rachis and delayed cellularization of oocytes in *glp-1* reduction-of-function mutants (Nadarajan *et al.* 2009).

On the somatic side, INX-8 and -9 appear to function redundantly: single mutants have no apparent fertility defects, and either gene alone rescues *inx-8 inx-9* double mutants. For the phenotypes described here—defects in germline proliferation, gametogenesis, the inhibition of meiotic maturation in the absence of sperm, and early embryogenesis—INX-8 and -9 are implicated as the somatic partners to the germline innexins.

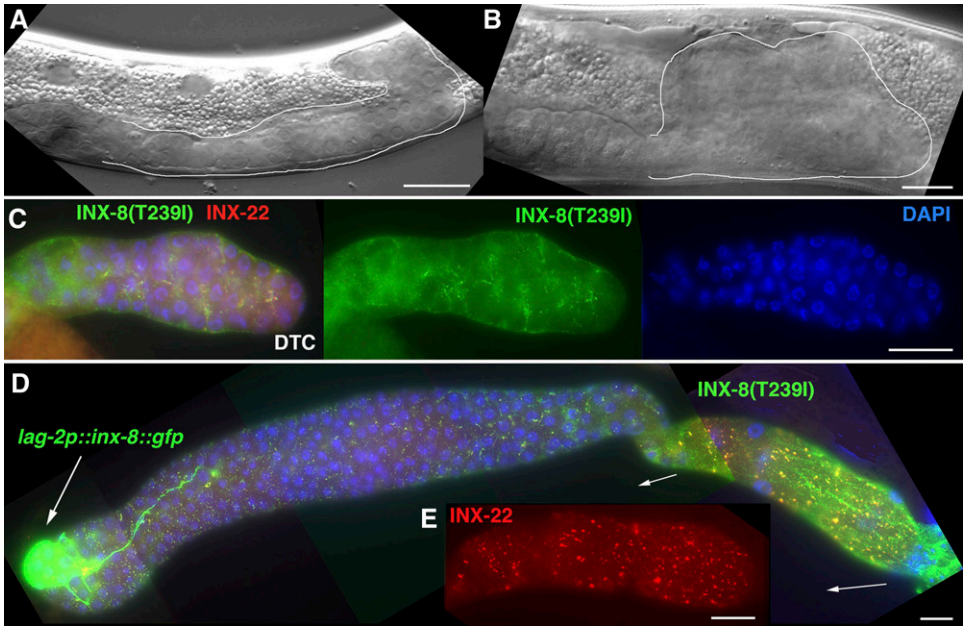

Figure 17 The *inx-8(tn1513)* mutation is hypomorphic. (A) *sem-3(n1655) inx-8(tn1513) inx-9(ok1502)* L4 animal showing production of ~30 germ cells in a single gonad arm; in adults, germ cells seldom become necrotic but become difficult to distinguish (B). (C) Rarely, a *sem-3 (n1655) inx-8(tn1513) inx-9(ok1502)* gonad arm can be dissected from L4 animals, and expression of INX-8(T239I) appears to colocalize with INX-22. (D and E) *sem-3(n1655) inx-8(tn1513) inx-9(ok1502)* animals rescued for germ cell proliferation with *lag-2p::inx-8::gfp* show colocalization of INX-22 and INX-8(T239I) in puncta in the proximal arm. DAPI staining of nuclei is shown in blue. Bars, 20 μm.

In addition to facilitating intercellular passage of small molecules, connexin and innexin family members have been proposed to contribute to cell adhesion or to function as hemichannels distinct from intercellular channels. A hemichannel role for the mutant phenotypes that we describe is unlikely because somatic and germline innexins exhibit essentially the same mutant phenotypes. Additionally, the dependence on INX-22 of somatic INX-8/9 endocytosis into ovulating oocytes suggests that these innexins form intercellular channels. A strictly adhesive role for these five innexins seems unlikely. In *inx-21(tn1540)* mutants, INX-22 might be expected to associate with INX-14 and dock with somatic hemichannels. Additionally, *inx-8(tn1513) inx-9(ok1502)* mutants produce an INX-8(T239I) product that appears capable of forming homomeric hemichannels that dock with INX-22/INX-14 hemichannels in the germ line. Thus a function that is strictly adhesive would appear to be fulfilled by INX-8(T239I). Rather, the limited amount of germline proliferation supported by INX-8(T239I) is likely due to a compromised channel function.

The requirement of soma–germline gap junctions for germline proliferation and gametogenesis

The lack of germ cells in *inx-8(tn1474) inx-9(ok1502)*, *inx-14(tm2864)*, and *inx-21(tn1540)* animals is reminiscent of *Drosophila melanogaster zero population growth* (*zpg*) mutants, which have greatly reduced germ cell numbers (Tazuke *et al.* 2002; Gilboa *et al.* 2003). The *zpg* locus encodes the germline-expressed Innexin 4 protein. *zpg* mutant germ cells were proposed to have defects in germ cell differentiation and survival. Examination of early stage gonads in *inx-8(tn1474) inx-9(ok1502)* animals indicated that germ cells fail to proliferate in these mutants. A few germ cell divisions may occur in a given animal, but evidence of meiotic entry or gametogenesis is not observed. *inx-8 inx-9* mutant germ cells may persist into later larval stages, but they appear to become necrotic in adults. The failure of germ cells to undergo gametogenesis in *inx-8(tn1474) inx-9(ok1502)* double mutants may be a secondary consequence of the proliferation defect. Clear parallels can be drawn with *zpg* germ cells, and it is possible that innexins in both systems may mediate similar functions.

A recent elegant study using genetic mosaics in *Drosophila* showed that GDP-L-fucose, required for the *O*-fucosylation of the extracellular Notch EGF-like repeats that regulate ligand binding, can be supplied through gap junctions composed of Innexin 2 (Ayukawa *et al.* 2012). Although it is possible that GDP-L-fucose might transit through INX-8/9: INX-14/21 channels, it is unlikely that a fucose deficiency for GLP-1/Notch signaling is the reason germ cells fail to proliferate in *inx-8(tn1474) inx-9(ok1502)* mutants. Epistasis tests with other mutations affecting germline proliferation showed that *inx-8(tn1474) inx-9(ok1502)* is epistatic to both loss-of-function *glp-1(q46)* and gain-of-function, ligand-independent *glp-1(oz112)* mutations, as well as *gld-2 gld-1* mutations that form germ cell tumors in a *glp-1*-independent manner. Therefore, loss of INX-8/9-based junctions prevents GLP-1/Notch-dependent, as well as GLP-1/Notch-independent, germline proliferation and differentiation.

Germline proliferation in *inx-8(tn1474) inx-9(ok1502)* mutants could largely be rescued by expression of INX-8::GFP in the DTC. The cellular processes of the DTC make extensive contacts with germ cells (Fitzgerald and Greenwald 1995; Hall *et al.* 1999; Byrd *et al.* 2014). Our analysis of the expression of gonadal innexins suggests that these processes are sites of extensive gap junction coupling between the DTC and germ cells, despite the individual junctions being too small to be seen in conventional thin sections by TEM. Possibly germ cells are coupled to the soma for most of their postembryonic development. As a germ cell

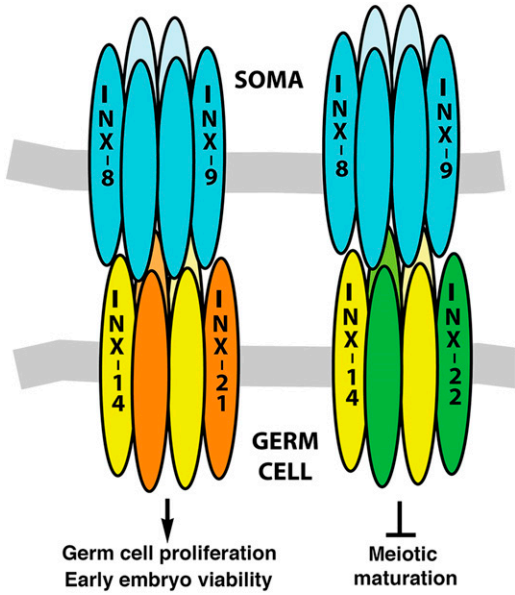

Figure 18 Model of innexin interactions in the gonad.

loses contact with the DTC, it might soon thereafter establish gap junctions with the sheath or sheath precursors. Processes from the DTC, sheath, and their earlier precursors might be more extensive than previously appreciated (*e.g.*, see Figure S3). Freeze-fracture analysis showed that gap junctions in this region of the distal arm are composed of loosely aggregated particles. As germ cells progress along the gonad arm, these contacts must be constantly altered, which might account for the general absence of large gap junction foci as observed in the proximal arm. The half-lives of connexins are generally on the order of 1–5 hr (Fallon and Goodenough 1981; Laird *et al.* 1991). Similar studies have not been carried out on innexins, and it is unknown if junctions between sheath and germ line are continually turned over and renewed, or if there is stability to these associations. Although our data support the existence of at least two classes of gap junction channels (with INX-14/21 or INX-14/22 hemichannels), the localization patterns of INX-21 and INX-22 always overlap, suggesting that different channel subunit combinations localize to the same general membrane domains. A recent study suggests that the membrane domains of nascent connexin43 gap junction formation (formation plaques) may differ in cholesterol composition from other membrane regions (Johnson *et al.* 2012). If such is the case for innexins, there may be a cooperative effect for gap junction formation between gap junction channels of different composition.

Two lines of evidence suggest that, in addition to the DTC, other somatic cells contribute to the proliferation function of soma–germline gap junctions. Genetic mosaic analysis showed that a rescuing *inx-8(+) inx-9(+)* extrachromosomal array could be lost from the DTC in a gonad arm that exhibited germline proliferation and that a *lim-7p*::*inx-8*::*gfp* construct, whose expression appears to be restricted to sheath cells and is first detected in the L3 stage, can also rescue proliferation to varying degrees. In a seminal study of interactions between soma and germ cells, McCarter *et al.* (1997) used laser ablations to eliminate specific somatic gonad cells. When both sheath-spermatheca (SS) precursor cells of a gonad arm were eliminated at the L2/L3 stage, the resultant number of germ cells (435 ± 10) was similar to what we obtained by expressing INX-8::GFP in the DTCs of *inx-8(tn1474) inx-9(ok1502)* mutants (523 ± 5). Therefore, it appears likely that, to achieve a wild-type level of germline proliferation, INX-8/9 must be expressed in the DTC as well as in other somatic cells, and the proliferation defects seen by SS laser ablation may reflect principally the loss of gap junction coupling between soma and the germ line.

Differences in germ cell behavior between a *glp-1(null)* mutation and DTC ablation in L1 stage animals were reported (Kimble and White 1981; Austin and Kimble 1989). Germ cells enter meiosis at the normal time following ablation of both DTCs, but germ cells enter meiosis one stage earlier in *glp-1(null)* mutants (Kimble and White 1981; Austin and Kimble 1989). One explanation for this difference is that GLP-1/Notch might be required to inhibit entry into the meiotic pathway of development in addition to promoting germ cell proliferation. Laser ablations revealed that cells of the somatic gonad other than the DTC are capable of inhibiting meiotic entry by providing GLP-1/Notch ligands (Pepper *et al.* 2003). Therefore, when the DTC is ablated, some GLP-1/Notch signaling is retained, and thus germ cells enter meiosis at the appropriate time. In *glp-1(null)* mutants, functional gap junctions between DTC and germ cells are retained. In contrast, laser ablation is predicted to eliminate DTC INX-8/9:INX-14/21 gap junctions, which support entry into the meiotic pathway of development. Possibly, germ cells in DTC-ablated L1s must later reestablish gap junctions with other cells of the somatic gonad to be able to enter meiosis, thus contributing to a delay in meiotic entry compared to *glp-1(null)* mutants.

Gap junctions as a defining feature of soma–germline interactions

Studies in mammalian systems support important reproductive functions for gap junctions in both females and males. Gap junctions between oocytes and cumulus cells (Anderson and Albertini 1976) play a critical role in the regulation of meiotic maturation in mammals (reviewed by Conti *et al.* 2012). cGMP moves through cumulus-oocyte connexin37 gap junctions to maintain meiotic arrest; luteinizing hormone triggers meiotic maturation in part through reducing the transmission of cGMP to the oocyte (Norris *et al.* 2008, 2009; Vaccari *et al.* 2008; Robinson *et al.* 2012; Zhang *et al.* 2012). Somatic cells of the follicle also supply nutrients, signals, and other metabolites to oocytes via gap junctions (Heller and Schultz 1980; Heller *et al.* 1981; Brower and Schultz 1982; Haghighat and van Winkle 1990; Downs *et al.* 1988). Connexin37 gap junctions are needed for oocyte growth and the acquisition of meiotic competence (Simon *et al.* 1997; Carabatsos *et al.* 2000), yet the molecular basis

for these requirements is uncertain. Gap junctions may play an early role in primordial germ cell (PGC) development in mammals: migrating PGCs in connexin43 mutant mice undergo apoptosis at about the time they arrive at the genital ridge (Juneja *et al.* 1999; Francis and Lo 2006). In the testis, Sertoli cells form gap junctions with germ cells (Russell 1980), and a Sertoli cell-specific knockout of connexin43 disrupts spermatogenesis (Brehm *et al.* 2007; Sridharan *et al.* 2007).

Our analysis reveals extensive roles for gap junctions in soma–germline interactions in *C. elegans*. The phenotypes that we describe may reflect a germline requirement for small molecules provided by the soma, but other scenarios are possible. For example, it is possible that germ cells might need to eliminate inhibitory factors or toxic metabolic products into the soma. Although we imagine that multiple classes of molecules may pass through these channels, there must be some level of specificity as exemplified by the different functions of INX-14/INX-21 and INX-14/22 hemichannels. Possibly only one of many molecules that pass through these channels is critical for a given function at a given time, or a class of similarly charged molecules may be gated in a manner that affects membrane potential (reviewed by Levin 2007). The small molecules that transit through invertebrate and vertebrate gap junctions might be very similar. Thus, the ability to genetically dissect the multiple gap junction functions underlying soma–germline interactions in *C. elegans* could have wide relevance for reproductive biology.

Acknowledgments

We thank Jane Hubbard, Shohei Mitani, and Tim Schedl for providing strains and/or reagents. Ed Hedgecock provided technical assistance and Chris Crocker contributed the illustration of the DTC. Some strains were provided by the Caenorhabditis Genetics Center, which is funded by grant P40OD010440 from the National Institutes of Health (NIH) Office of Research Infrastructure Programs. Electron microscopy was carried out with the assistance of Robert Hafner in the Characterization Facility at the University of Minnesota, which receives partial support from the National Science Foundation through the Materials Research Science and Engineering Center program. We thank Jane Hubbard, Tim Schedl, and Caroline Spike for their many helpful suggestions during the course of this work. This work was supported by NIH grants GM57173 and GM65115 (to D.G.) and OD010943 (to D.H.H.).

Literature Cited

Altun, Z. F., B. Chen, Z.-W. Wang, and D. H. Hall, 2009 High resolution map of *Caenorhabditis elegans* gap junction proteins. Dev. Dyn. 238: 1936–1950.

Anderson, E., and D. F. Albertini, 1976 Gap junctions between the oocyte and companion follicle cells in the mammalian ovary. J. Cell Biol. 71: 680–686.

Austin, J., and J. Kimble, 1987 *glp-1* is required in the germ line for regulation of the decision between mitosis and meiosis in *C. elegans*. Cell 51: 589–599.

Austin, J., and J. Kimble, 1989 Transcript analysis of *glp*-1 and *lin-12*, homologous genes required for cell interactions during development of *C. elegans*. Cell 58: 565–571.

Ayukawa, T., K. Matsumoto, H. O. Ishikawa, A. Ishio, T. Yamakawa *et al.*, 2012 Rescue of *Notch* signaling in cells incapable of GDP-L-fucose synthesis by gap junction transfer of GDP-L-fucose in *Drosophila*. Proc. Natl. Acad. Sci. USA 109: 15318–15323.

Baerwald, R. J., 1975 Inverted gap and other cell junctions in cockroach hemocyte capsules: a thin section and freeze-fracture study. Tissue Cell 7: 575–585.

Berry, L. W., B. Westlund, and T. Schedl, 1997 Germ-line tumor formation caused by activation of *glp-1*, a *Caenorhabditis elegans* member of the *Notch* family of receptors. Development 124: 925–936.

Blumenthal, T., 2012 Trans-splicing and operons in *C. elegans* (November 20, 2012), WormBook, ed. The *C. elegans* Research Community, WormBook, doi/10.1895/wormbook.1.5.2, http://www.wormbook.org.

Brehm, R., M. Zeiler, C. Rüttlinger, K. Herde, M. Kibschull *et al.*, 2007 A sertoli cell-specific knockout of connexin43 prevents initiation of spermatogenesis. Am. J. Pathol. 171: 19–31.

Brower, P. T., and R. T. Schultz, 1982 Intercellular communication between granulosa cells and mouse oocytes: existence and possible nutritional role during oocyte growth. Dev. Biol. 90: 144–153.

Byrd, D. T., K. Knobel, K. Affeldt, S. L. Crittenden, and J. Kimble, 2014 A DTC niche plexus surrounds the germline stem cell pool in *Caenorhabditis elegans*. PLoS ONE 9: e88372.

Carabatsos, M. J., C. Sellitto, D. A. Goodenough, and D. F. Albertini, 2000 Oocyte-granulosa cell heterologous gap junctions are required for the coordination of nuclear and cytoplasmic meiotic competence. Dev. Biol. 226: 167–179.

Cheng, H., J. A. Govindan, and D. Greenstein, 2008 Regulated trafficking of the MSP/Eph receptor during oocyte meiotic maturation in *C. elegans*. Curr. Biol. 18: 705–714.

Christensen, S., V. Kodoyianni, M. Bosenberg, L. Friedman, and J. Kimble, 1996 *lag-1*, a gene required for *lin-12* and *glp*-1 signaling in *Caenorhabditis elegans*, is homologous to human CBF1 and Drosophila Su(H). Development 122: 1373–1383.

Conti, M., M. Hsieh, A. M. Zamah, and J. S. Oh, 2012 Novel signaling mechanisms in the ovary during oocyte maturation and ovulation. Mol. Cell. Endocrinol. 356: 65–73.

Dalfó, D., D. Michaelson, and E. J. Hubbard, 2012 Sensory regulation of the *C. elegans* germline through TGF-β-dependent signaling in the niche. Curr. Biol. 22: 712–719.

Dickinson, D. J., J. D. Ward, D. J. Reiner, and B. Goldstein, 2013 Engineering the *Caenorhabditis elegans* genome using Cas9-triggered homologous recombination. Nat. Methods 10: 1028–1034.

Doh, J. H., Y. Jung, V. Reinke, and M.-H. Lee, 2013 *C. elegans* RNA-binding protein GLD-1 recognizes its multiple targets using sequence, context, and structural information to repress translation. Worm 2: e26548.

Downs, S. M., S. A. Daniel, and J. J. Eppig, 1988 Induction of maturation in cumulus cell-enclosed mouse oocytes by follicle-stimulating hormone and epidermal growth factor: evidence for a positive stimulus of somatic origin. J. Exp. Zool. 245: 86–96.

Doyle, T. G., C. Wen, and I. Greenwald, 2000 SEL-8, a nuclear protein required for LIN-12 and GLP-1 signaling in *Caenorhabditis elegans*. Proc. Natl. Acad. Sci. USA 97: 7877–7881.

Edmonds, J. W., S. L. McKinney, J. K. Prasain, and M. A. Miller, 2011 The gap junctional protein INX-14 functions in oocyte precursors to promote *C. elegans* sperm guidance. Dev. Biol. 359: 47–58.

Fallon, R. F., and D. A. Goodenough, 1981 Five-hour half-life of mouse liver gap-junction protein. J. Cell Biol. 90: 521–526.

Finney, M., and G. Ruvkun, 1990 The *unc-86* gene product couples cell lineage and cell identity in *C. elegans*. Cell 63: 895–905.

Fitzgerald, K., and I. Greenwald, 1995 Interchangeability of *Caenorhabditis elegans* DSL proteins and intrinsic signalling activity of their extracellular domains in vivo. Development 123: 4275–4282.

Flower, N. E., 1972 A new junctional structure in the epithelia of insects of the order Dictyoptera. J. Cell Sci. 10: 683–691.

Flower, N. E., 1977 Invertebrate gap junctions. J. Cell Sci. 25: 163–171.

Francis, R. J., and C. W. Lo, 2006 Primordial germ cell deficiency in the connexin 43 knockout mouse arises from apoptosis associated with abnormal p53 activation. Development 133: 3451–3460.

Francis, R., E. Maine, and T. Schedl, 1995a Analysis of the multiple roles of *gld-1* in germline development: interactions with the sex determination cascade and the *glp-1* signaling pathway. Genetics 139: 607–630.

Francis, R., M. K. Barton, J. Kimble, and T. Schedl, 1995b *gld-1*, a tumor suppressor gene required for oocyte development in *Caenorhabditis elegans*. Genetics 139: 579–606.

Friedland, A. E., Y. B. Tzur, K. M. Esvelt, M. P. Colaiácovo, G. M. Church *et al.*, 2013 Heritable genome editing in *C. elegans* via a CRISPR-Cas9 system. Nat. Methods 10: 741–743.

Gilboa, L., A. Forbes, S. I. Tazuke, M. T. Fuller, and R. Lehmann, 2003 Germ line stem cell differentiation in Drosophila requires gap junctions and proceeds via an intermediate state. Development 130: 6625–6634.

Goodenough, D. A., and J. P. Revel, 1970 Fine structural analysis of intercellular junctions in the mouse liver. J. Cell Biol. 45: 272–290.

Govindan, J. A., H. Cheng, J. E. Harris, and D. Greenstein, 2006 $G\alpha_{o/i}$ and $G\alpha_s$ signaling function in parallel with the MSP/Eph receptor to control meiotic diapause in *C. elegans*. Curr. Biol. 16: 1257–1268.

Govindan, J. A., S. Nadarajan, S. Kim, T. A. Starich, and D. Greenstein, 2009 Somatic cAMP signaling regulates MSP-dependent oocyte growth and meiotic maturation in *C. elegans*. Development 136: 2211–2221.

Haghighat, N., and L. J. van Winkle, 1990 Developmental change in follicular cell-enhanced amino acid uptake into mouse oocytes depends on intact gap junctions and transport system Gly. J. Exp. Zool. 253: 71–82.

Hall, D. H., 1992 Freeze-fracture and freeze-etch studies of the nematode, *Caenorhabditis elegans*. Ann. N. Y. Acad. Sci. 494: 215–217.

Hall, D. H., 1995 Electron microscopy and three-dimensional image reconstruction. Methods Cell Biol. 48: 395–436.

Hall, D. H., V. P. Winfrey, G. Blaeuer, L. H. Hoffman, T. Furuta *et al.*, 1999 Ultrastructural features of the adult hermaphrodite gonad of *Caenorhabditis elegans*: relations between the germ line and soma. Dev. Biol. 212: 101–123.

Hansen, D., and T. Schedl, 2013 Stem cell proliferation *vs.* meiotic fate decision in *Caenorhabditis elegans*. Adv. Exp. Med. Biol. 757: 71–99.

Hansen, D., E. J. Hubbard, and T. Schedl, 2004a Multi-pathway control of the proliferation *vs.* meiotic development decision in the *Caenorhabditis elegans* germline. Dev. Biol. 268: 342–357.

Hansen, D., L. Wilson-Berry, T. Dang, and T. Schedl, 2004b Control of the proliferation *vs.* meiotic development decision in the *C. elegans* germline through the regulation of GLD-1 protein accumulation. Development 131: 93–104.

Harris, J. E., J. A. Govindan, I. Yamamoto, J. Schwartz, I. Kaverina *et al.*, 2006 Major sperm protein signaling promotes oocyte microtubule reorganization prior to fertilization in *Caenorhabditis elegans*. Dev. Biol. 299: 105–121.

Heller, D. T., and R. T. Schultz, 1980 Ribonucleotide metabolism by mouse oocytes: metabolic cooperativity between the fully grown oocyte and cumulus cells. J. Exp. Zool. 214: 355–364.

Heller, D. T., D. M. Cahill, and R. T. Schultz, 1981 Biochemical studies of mammalian oogenesis: metabolic cooperativity between granulosa cells and growing mouse oocytes. Dev. Biol. 84: 455–464.

Henderson, S. T., D. Gao, E. J. Lambie, and J. Kimble, 1994 *lag-2* may encode a signaling ligand for the GLP-1 and LIN-12 receptors of *C. elegans*. Development 120: 2913–2924.

Hubbard, E. J., and D. Greenstein, 2000 The *Caenorhabditis elegans* gonad: a test tube for cell and developmental biology. Dev. Dyn. 218: 2–22.

Hubbard, E. J., D. Z. Korta, and D. Dalfó, 2013 Physiological control of germline development. Adv. Exp. Med. Biol. 757: 101–131.

Jan, E., C. K. Motzny, L. E. Graves, and E. B. Goodwin, 1999 The STAR protein, GLD-1, is a translational regulator of sexual identity in *Caenorhabditis elegans*. EMBO J. 18: 258–269.

Jantsch-Plunger, V., and M. Glotzer, 1999 Depletion of syntaxins in the early *Caenorhabditis elegans* embryo reveals a role for membrane fusion events in cytokinesis. Curr. Biol. 9: 738–745.

Johnson, R. G., J. K. Reynhout, E. M. TenBroek, B. J. Quade, T. Yasumura *et al.*, 2012 Gap junction assembly: roles for the formation plaque and regulation by the C-terminus of connexin43. Mol. Biol. Cell 23: 71–86.

Johnston, W. L., A. Krizus, and J. W. Dennis, 2006 The eggshell is required for meiotic fidelity, polar-body extrusion and polarization of the *C. elegans* embryo. BMC Biol. 4: 35.

Jones, A. R., and T. Schedl, 1995 Mutations in *gld-1*, a female germ cell-specific tumor suppressor gene in *Caenorhabditis elegans*, affects a conserved domain also found in Src-associated protein Sam68. Genes Dev. 9: 1491–1504.

Jordan, K., R. Chodock, A. R. Hand, and D. W. Laird, 2001 The origin of annular junctions: a mechanism of gap junction internalization. J. Cell Sci. 114: 763–773.

Jud, M. C., M. J. Czerwinski, M. P. Wood, R. A. Young, C. M. Gallo *et al.*, 2008 Large P body-like RNPs form in *C. elegans* oocytes in response to arrested ovulation, heat shock, osmotic stress, and anoxia and are regulated by the major sperm protein pathway. Dev. Biol. 318: 38–51.

Juneja, S. C., K. J. Barr, G. C. Enders, and G. M. Kidder, 1999 Defects in the germ line and gonads of mice lacking connexin43. Biol. Reprod. 60: 1263–1270.

Jungkamp, A. C., M. Stoeckius, D. Mecenas, D. Grün, G. Mastrobuoni *et al.*, 2011 *In vivo* and transcriptome-wide identification of RNA binding protein target sites. Mol. Cell 44: 828–840.

Kadyk, L. C., and J. Kimble, 1998 Genetic regulation of entry into meiosis in *Caenorhabditis elegans*. Development 125: 1803–1813.

Kawasaki, I., Y.-H. Shim, J. Kirchner, W. B. Wood, and S. Strome, 1998 PGL-1, a predicted RNA-binding component of germ granules, is essential for fertility in *C. elegans*. Cell 94: 635–645.

Kershner, A. M., H. Shin, T. J. Hansen, and J. Kimble, 2014 Discovery of two GLP-1/Notch target genes that account for the role of GLP-1/Notch signaling in stem cell maintenance. Proc. Natl. Acad. Sci. USA 111: 3739–3744.

Killian, D. J., and E. J. A. Hubbard, 2005 *Caenorhabditis elegans* germline patterning requires coordinated development of the somatic gonad sheath and the germ line. Dev. Biol. 279: 322–335.

Kim, K. W., T. L. Wilson, and J. Kimble, 2010 GLD-2/RNP-8 cytoplasmic poly(A) polymerase is a broad-spectrum regulator of the oogenesis program. Proc. Natl. Acad. Sci. USA 107: 17445–17450.

Kim, S., J. A. Govindan, Z. J. Tu, and D. Greenstein, 2012 SACY-1 DEAD-Box helicase links the somatic control of oocyte meiotic maturation to the sperm-to-oocyte switch and gamete maintenance in *Caenorhabditis elegans*. Genetics 192: 905–928.

Kimble, J., and S. L. Crittenden, 2007 Controls of germline stem cells, entry into meiosis, and the sperm/oocyte decision in *Caenorhabditis elegans*. Annu. Rev. Cell Dev. Biol. 23: 405–433.

Kimble, J., and D. Hirsh, 1979 The postembryonic cell lineages of the hermaphrodite and male gonads in *Caenorhabditis elegans*. Dev. Biol. 70: 396–417.

Kimble, J., and J. G. White, 1981 On the control of germ cell development in *Caenorhabditis elegans*. Dev. Biol. 81: 208–219.

Korta, D. Z., S. Tuck, and E. J. Hubbard, 2012 S6K links cell fate, cell cycle and nutrient response in *C. elegans* germline stem/progenitor cells. Development 139: 859–870.

Laird, D. W., K. L. Puranam, and J.-P. Revel, 1991 Turnover and phosphorylation dynamics of connexin43 gap junction protein in cultured cardiac myocytes. Biochem. J. 273: 67–72.

Land, M., A. Islas-Trejo, and C. S. Rubin, 1994 Origin, properties, and regulated expression of multiple mRNAs encoded by the protein kinase C1 gene of *Caenorhabditis elegans*. J. Biol. Chem. 269: 14820–14827.

Larsen, W. J., H. N. Tung, S. A. Murray, and C. A. Swenson, 1979 Evidence for the participation of actin microfilaments and bristle coats in the internalization of gap junction membrane. J. Cell Biol. 83: 576–587.

Lee, M.-H., and T. Schedl, 2001 Identification of in vivo mRNA targets of GLD-1, a maxi-KH motif containing protein required for *C. elegans* germ cell development. Genes Dev. 15: 2408–2420.

Lee, M.-H., M. Ohmachi, S. Arur, S. Nayak, R. Francis *et al.*, 2007 Multiple functions and dynamic activation of MPK-1 ERK signaling in *Caenorhabditis elegans* germline development. Genetics 177: 2039–2062.

Levin, M., 2007 Gap junctional communication in morphogenesis. Prog. Biophys. Mol. Biol. 94: 186–206.

McCarter, J., B. Bartlett, T. Dang, and T. Schedl, 1997 Soma-germ cell interactions in *Caenorhabditis elegans*: multiple events of hermaphrodite germline development require the somatic sheath and spermathecal lineages. Dev. Biol. 181: 121–143.

McCarter, J., B. Bartlett, T. Dang, and T. Schedl, 1999 On the control of oocyte meiotic maturation and ovulation in *C. elegans*. Dev. Biol. 205: 111–128.

Michaelson, D., D. Z. Korta, Y. Capua, and E. J. Hubbard, 2010 Insulin signaling promotes germline proliferation in *C. elegans*. Development 137: 671–680.

Miller, M. A., V. Q. Nguyen, M.-H. Lee, M. Kosinski, T. Schedl *et al.*, 2001 A sperm cytoskeletal protein that signals oocyte meiotic maturation and ovulation. Science 291: 2144–2147.

Miyata, S., J. Bergun, E. R. Troemel, and F. M. Ausubel, 2008 DAF-16-dependent suppression of immunity during reproduction in *Caenorhabditis elegans*. Genetics 178: 903–918.

Nadarajan, S., J. A. Govindan, M. McGovern, E. J. A. Hubbard, and D. Greenstein, 2009 MSP and GLP-1/Notch signaling coordinately regulate actomyosin-dependent cytoplasmic streaming and oocyte growth in *C. elegans*. Development 136: 2223–2234.

Narbonne, P., and R. Roy, 2006 Inhibition of germline proliferation during *C. elegans* dauer development requires PTEN, LKB1 and AMPK signaling. Development 133: 611–619.

Nielsen, M. S., L. N. Axelsen, P. L. Sorgen, V. Verma, M. Delmar *et al.*, 2012 Gap junctions. Compr. Physiol. 2: 1981–2035.

Norris, R. P., M. Freudzon, L. M. Mehlmann, A. E. Cowan, A. M. Simon *et al.*, 2008 Luteinizing hormone causes MAP kinase-dependent phosphorylation and closure of connexin 43 gap junctions in mouse ovarian follicles: one of two paths to meiotic resumption. Development 135: 3229–3238.

Norris, R. P., W. J. Ratzan, M. Freudzon, L. M. Mehlmann, J. Krall *et al.*, 2009 Cyclic GMP from the surrounding somatic cells regulates cyclic AMP and meiosis in the mouse oocyte. Development 136: 1869–1878.

Oatley, J. M., and R. L. Brinster, 2012 The germline stem cell niche unit in mammalian testes. Physiol. Rev. 92: 577–595.

Olson, S. K., J. R. Bishop, J. R. Yates, K. Oegema, and J. D. Esko, 2006 Identification of novel chondroitin proteoglycans in *Caenorhabditis elegans*: embryonic cell division depends on CPG-1 and CPG-2. J. Cell Biol. 173: 985–994.

Olson, S. K., G. Greenan, A. Desai, T. Müller-Reichert, and K. Oegema, 2012 Hierarchical assembly of the eggshell and permeability barrier in *C. elegans*. J. Cell Biol. 198: 731–748.

Pepper, A. S.-R., T.-W. Lo, D. J. Killian, D. H. Hall, and E. J. A. Hubbard, 2003 The establishment of *Caenorhabditis elegans* germline pattern is controlled by overlapping proximal and distal somatic gonad signals. Dev. Biol. 259: 336–350.

Petcherski, A. G., and J. Kimble, 2000 LAG-3 is a putative transcriptional activator in the *C. elegans* Notch pathway. Nature 405: 364–368.

Piehl, M., C. Lehmann, A. Gumpert, J.-P. Denizot, D. Segretain *et al.*, 2007 Internalization of large double-membrane intercellular vesicles by a clathrin-dependent endocytic process. Mol. Biol. Cell 18: 337–347.

Rash, J. E., and C. Hudson, 1979 *Freeze Fracture: Methods, Artifacts, and Interpretations*. Raven Press, New York.

Robinson, J. W., M. Zhang, L. C. Shuhaibar, R. P. Norris, A. Geerts *et al.*, 2012 Luteinizing hormone reduces the activity of NPR2 guanylyl cyclase in mouse ovarian follicles, contributing to the cyclic GMP decrease that promotes resumption of meiosis in oocytes. Dev. Biol. 366: 308–316.

Russell, L. D., 1980 Sertoli-germ cell interrelations: a review. Gamete Res. 3: 179–202.

Schedl, T., and J. Kimble, 1988 *fog-2*, a germ-line-specific sex determination gene required for hermaphrodite spermatogenesis in *Caenorhabditis elegans*. Genetics 119: 43–61.

Sertoli, E., 1865 Dell' esistenza di particolari cellule ramificate nei canalicoli seminiferi del testicolo umano. Morgagni 7: 31–40.

Simon, A. G., D. A. Goodenough, E. Li, and D. L. Paul, 1997 Female infertility in mice lacking connexin 37. Nature 385: 525–529.

Simonsen, K. T., D. G. Moerman, and C. C. Naus, 2014 Gap junctions in *C. elegans*. Front. Physiol. 5: 40.

Sridharan, S., L. Simon, D. D. Meling, D. G. Cyr, D. E. Gutstein *et al.*, 2007 Proliferation of adult sertoli cells following conditional knockout of the gap junctional protein GJA1 (connexin 43) in mice. Biol. Reprod. 76: 804–812.

Starich, T., M. Sheehan, J. Jadrich, and J. Shaw, 2001 Innexins in *C. elegans*. Cell Commun. Adhes. 8: 311–314.

Svingen, T., and P. Koopman, 2013 Building the mammalian testis: origins, differentiation, and assembly of the component cell populations. Genes Dev. 27: 2409–2426.

Swales, L. S., and N. J. Lane, 1985 Unusual structural features and assembly of gap and pleated septate junctions in embryonic cockroach CNS. J. Cell Sci. 76: 269–281.

Tax, F. E., J. J. Yeargers, and J. H. Thomas, 1994 Sequence of *C. elegans lag-2* reveals a cell-signaling domain shared with *Delta* and *Serrate* of *Drosophila*. Nature 368: 150–154.

Tax, F. E., J. H. Thomas, E. L. Ferguson, and H. R. Horvitz, 1997 Identification and characterization of genes that interact with *lin-12* in *Caenorhabditis elegans*. Genetics 147: 1675–1695.

Tazuke, S. I., C. Schulz, L. Gilboa, M. Fogarty, A. P. Mahowald *et al.*, 2002 A germline-specific gap junction protein required for survival of differentiating early germ cells. Development 129: 2529–2539.

Toya, M., Y. Iida, and A. Sugimoto, 2010 Imaging of mitotic spindle dynamics in *Caenorhabditis elegans* embryos. Methods Cell Biol. 97: 359–372.

Troeml, E. R., B. E. Kimmel, and C. I. Bargmann, 1997 Reprogramming chemotaxis responses: sensory neurons define olfactory preferences in *C. elegans*. Cell 91: 161–169.

Tzur, Y. B., A. E. Friedland, S. Nadarajan, G. M. Church, J. A. Calarco *et al.*, 2013 Heritable custom genomic modifications in *Caenorhabditis elegans* via a CRISPR-Cas9 system. Genetics 195: 1181–1185.

Vaccari, S., K. Horner, L. M. Mehlmann, and M. Conti, 2008 Generation of mouse oocytes defective in cAMP synthesis and degradation:

endogenous cyclic AMP is essential for meiotic arrest. Dev. Biol. 316: 124–134.

Voutev, R., R. Keating, E. J. Hubbard, and L. G. Vallier, 2009 Characterization of the *C. elegans Islet* LIM-homeodomain ortholog, *lim-7*. FEBS Lett. 583: 456–464.

Wang, L., C. R. Eckmann, L. C. Kadyk, M. Wickens, and J. Kimble, 2002 A regulatory cytoplasmic poly(A) polymerase in *Caenorhabditis elegans*. Nature 419: 312–316.

Ward, S., and J. S. Carrel, 1979 Fertilization and sperm competition in the nematode *Caenorhabditis elegans*. Dev. Biol. 73: 304–321.

Ward, S., Y. Argon, and G. A. Nelson, 1981 Sperm morphogenesis in wild-type and fertilization-defective mutants of *Caenorhabditis elegans*. J. Cell Biol. 91: 26–44.

Whitten, S. J., and M. A. Miller, 2007 The role of gap junctions in *Caenorhabditis elegans* oocyte maturation and fertilization. Dev. Biol. 301: 432–446.

Wright, J. E., D. Gaidartzis, M. Senften, B. M. Farley, E. Westhof *et al.*, 2011 A quantitative RNA code for mRNA target selection by the germline fate determinant GLD-1. EMBO J. 30: 533–545.

Yochem, J., and I. Greenwald, 1989 *glp-1* and *lin-12*, genes implicated in distinct cell-cell interactions in *Caenorhabditis elegans*, encode similar transmembrane proteins. Cell 58: 553–563.

Yochem, J., and R. K. Herman, 2003 Investigating *C. elegans* development through mosaic analysis. Development 130: 4781–4788.

Yochem, J., T. Gu, and M. Han, 1998 A new marker for mosaic analysis in *Caenorhabditis elegans* indicates a fusion between hyp6 and hyp7, two major components of the hypodermis. Genetics 149: 1323–1334.

Zhang, M., Y.-Q. Su, K. Sugiura, G. Xia, and J. J. Eppig, 2012 Granulosa cell ligand NPPC and its receptor NPR2 maintain meiotic arrest in mouse oocytes. Science 330: 366–369.

Zhang, Y., J. M. Foster, L. S. Nelson, D. Ma, and C. K. S. Carlow, 2005 The chitin synthase genes *chs-1* and *chs-2* are essential for *C. elegans* development and responsible for chitin deposition in the eggshell and pharynx, respectively. Dev. Biol. 285: 330–339.

Communicating editor: M. Sundaram

GENETICS

Supporting Information
http://www.genetics.org/lookup/suppl/doi:10.1534/genetics.114.168815/-/DC1

Two Classes of Gap Junction Channels Mediate Soma-Germline Interactions Essential for Germline Proliferation and Gametogenesis in *Caenorhabditis elegans*

Todd A. Starich, David H. Hall, and David Greenstein

DOI: 10.1534/genetics.114.168815

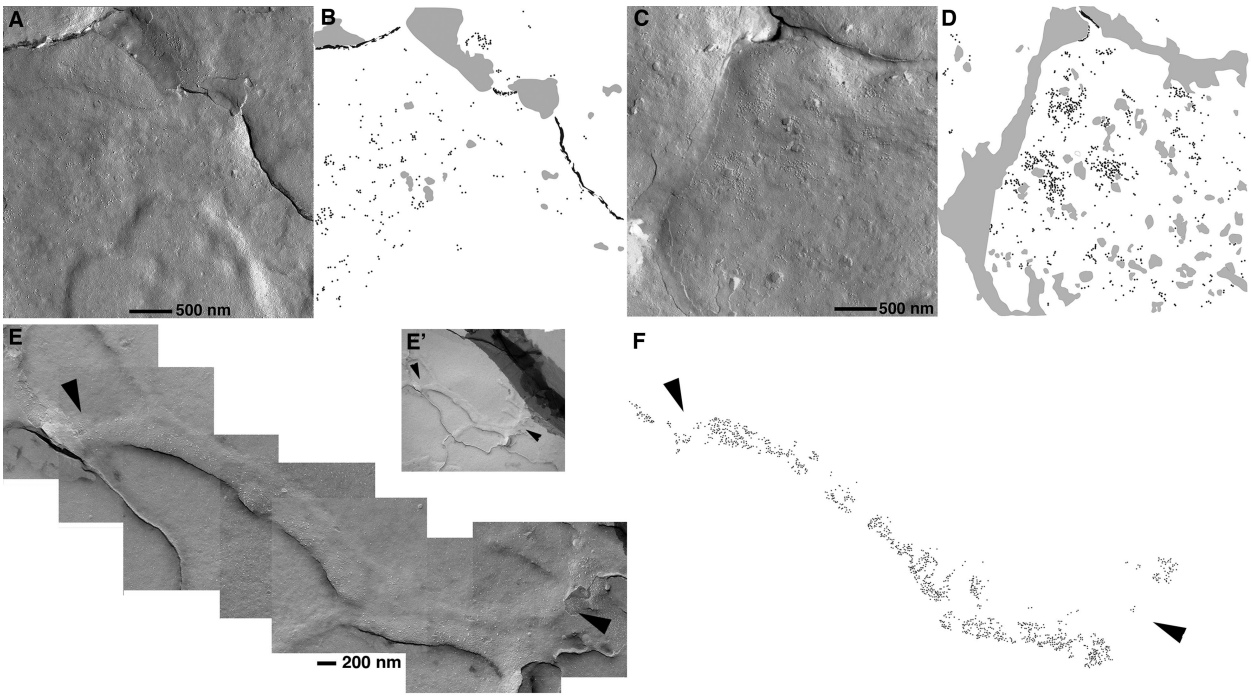

Figure S1 Freeze-fracture TEM images of arrangements of gap junction molecules on germ cell surfaces. (A) Low-magnification image to show distribution of loosely-aggregated large particles on the P-face of a germ cell. Several small clusters of particles may represent sites of nascent gap junction formation. (B) Diagram of (A) with particles indicated as black dots. (C, D) Second germ cell showing larger aggregations of particles. (E) Very large arrangement of pits on the E-face of the sheath, stretching across the entire length of a germ cell (arrowheads mark the limits of the sheath E-face profile). (E') Low-magnification image of (E). (F) Pits in (E) that likely correspond to gap junction particles are indicated with black dots.

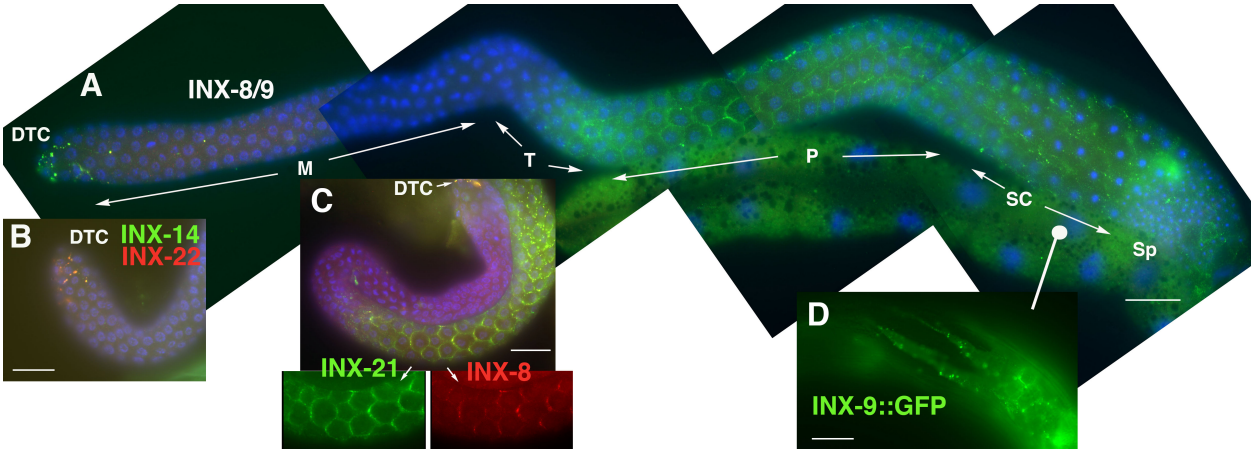

Figure S2 Distribution of innexins in the male gonad. (A) INX-8/9 is expressed in the DTCs, the pachytene region and the proximal arm. (B and C) Germ cell innexins colocalize with INX-8/9 in these same regions. (D) INX-9::GFP visualizes extensions of somatic cells in the region of the seminal vesicle. Scale bars, 20 µm.

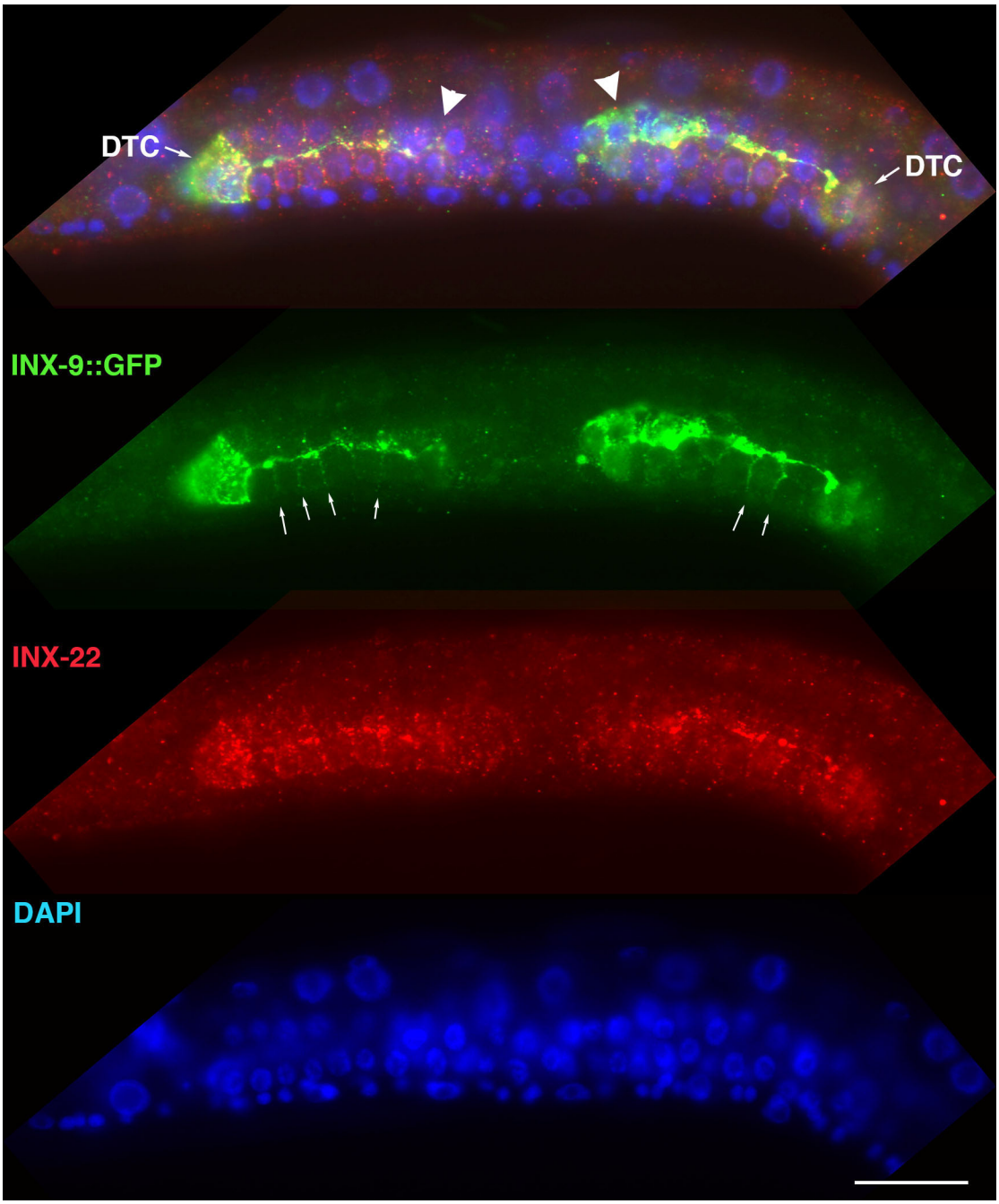

Figure S3 The DTC and other somatic cells establish gap junctions with most or all germ cells at the L2/L3 stage. A wild-type L2/L3 larva carrying *inx-9::gfp* was stained with anti-GFP and anti-INX-22 antibodies. A brightly-staining prominent process appears to emanate from each of the DTCs (the DTC associated with the right gonad arm lies out of this focal plane). As visualized in live animals, these large processes appear to run on the exterior surface of the germ cells, while other finer processes appear to radiate out from the large process and encircle the germ cells (small arrows). Other somatic gonad cells start to express *inx-9::gfp* at this time (arrowheads; cluster of cells in the left arm is just out of this focal plane), and it is unclear to what degree they may contribute to these processes. INX-22 and INX-9::GFP colocalize extensively along these processes; some tiny puncta can be detected along the finer processes, but their size suggests that gap junctions formed at this time may be small and masked by the strong diffuse expression signals detected for INX-9::GFP. Scale bar, 20 µm.

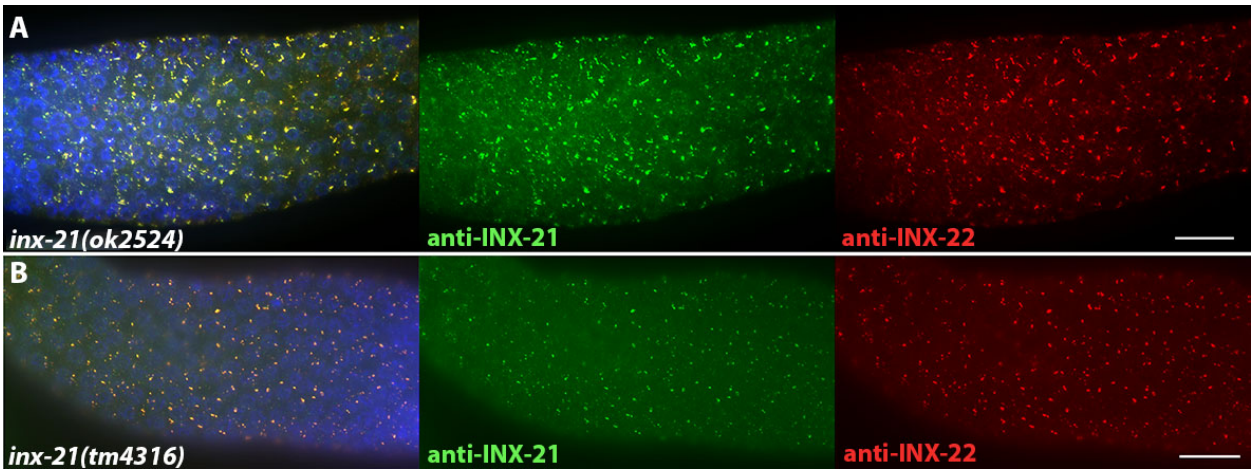

Figure S4 Anti-INX-21 antibodies detect punctate signals in *inx-21(ok2524)* (A) and *inx-21(tm4316)* (B) mutants that colocalize with INX-22. For technical reasons (i.e., *inx-21*null mutants are sterile and produce few germ cells), we cannot exclude the possibility that the anti-INX-21 sera cross reacts to some extent with INX-22 (the carboxyl termini of INX-21 and INX-22 share 26% identity). DAPI staining of nuclei is in blue. Scale bars, 20 µm.

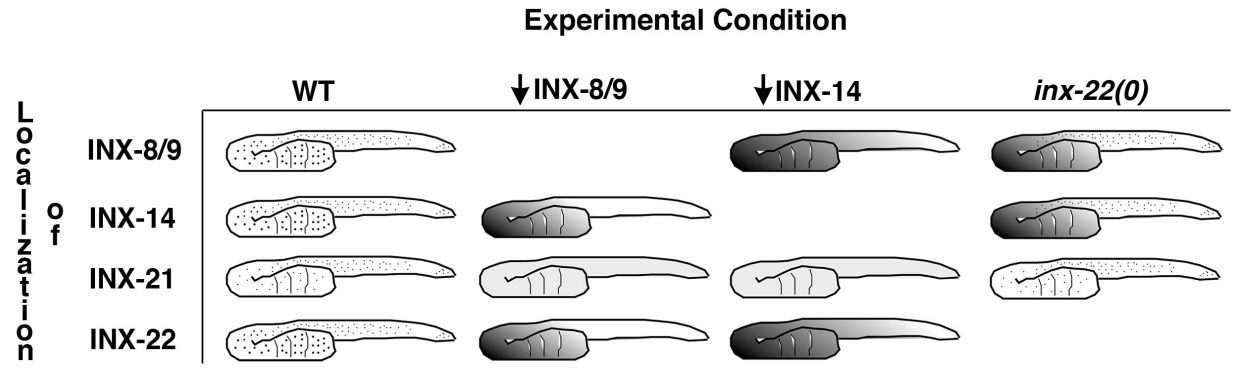

Figure S5 Summary of interdependence of innexin colocalization in the gonad. Because complete elimination of INX-8/9 or INX-14 produces gonad arms with few or no germ cells, we used experimental conditions to reduce expression of INX-8/9 and INX-14. These conditions included the examination of the hypomorphic *inx-14(ag17)* mutant, as well as animals that showed sufficient germ line proliferation to produce reflexed gonad arms after *inx-14(RNAi)* treatment of the wild type, or after *inx-8(RNAi)* treatment of *inx-9(ok1502)* mutants. In addition, we examined *inx-22(tm1661)* animals. An absence of innexin colocalization to puncta is interpreted as a reduction in gap junction formation. When puncta fail to form under these experimental conditions, expression of the non-targeted innexins can often be detected in a diffuse pattern (indicated as shading). Relatively high expression levels of INX-8/9, INX-14 and INX-22 in the proximal arm allow a strong signal to be detected even when diffuse, as indicated by darker shading; weaker diffuse expression in the distal arm, and for INX-21 throughout, is indicated as light shading.

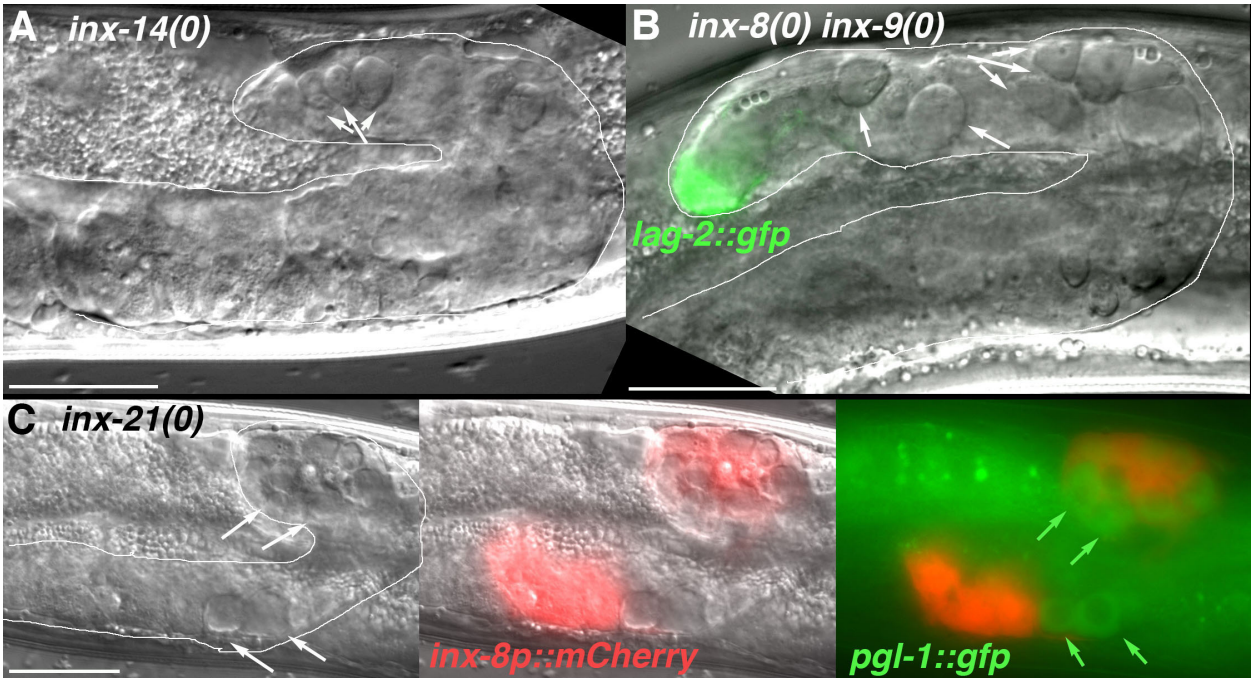

Figure S6 Germ cells in gonad innexin mutants become necrotic in adults. (A) *inx-14(tm2864)* gonad arm outlined, arrows point to a few of the necrotic foci. (B) *inx-8(tn1474) inx-9(ok1502)* with *lag-2::gfp* reporter marking the DTC and showing that germ cells, (arrows) but not the DTC, appear to undergo necrosis. (C) *inx-21(tn1540)* gonad arm expressing *inx-8p::mCherry* to visualize the DTC and sheath, and *pgl-1::gfp* to indicate germ cells. The distribution pattern of PGL-1::GFP is not particulate as in the wild type (see Figure 9C in the main text). Scale bars, 20 µm.

Table S1 UDP-GlcNac injections rescue *gna-2(qa705)* mutants but not *inx-8(tn1474) inx-9(ok1502); tnEx205[lag-2p::inx-8::gfp)* mutants

Genotype	[UDP-GlcNac] injected[a]	Average number of progeny[b]
gna-2(qa705) unc-55(e1170)	uninjected	0 ± 0 (n=16)
	250 mM	3.0 ± 2.3 (n=23)
inx-8(tn1474) inx-9(ok1502); tnEx205[lag-2p::inx-8::gfp)	uninjected	0.6 ± 0.8 (n=15)
	100 mM	0.7 ± 0.9 (n=16)
	250 mM	0.4 ± 0.6 (n=20)

[a]Adults were injected in a single gonad arm.
[b]The average number of hatched larvae.